

NASA CR

140290

AGRICULTURAL TERRAIN SCATTEROMETER OBSERVATIONS WITH EMPHASIS ON SOIL MOISTURE VARIATIONS

CRES Technical Report 177-44

C. King

(NASA-CF-140290) AGRICULTURAL TERRAIN
SCATTEROMETER OBSERVATIONS WITH EMPHASIS
ON SOIL MOISTURE VARIATIONS (Kansas Univ.
Center for Research, Inc.) 57 p HC
\$6.00

N74-34768

Unclass
49051

CSOL C&F G3/13

August, 1973

Supported by:

NATIONAL AERONAUTICS AND SPACE ADMINISTRATION
Lyndon B. Johnson Space Center
Houston, Texas 77058
CONTRACT NAS 9-10261



THE UNIVERSITY OF KANSAS CENTER FOR RESEARCH, INC.

2385 Irving Hill Rd.— Campus West Lawrence, Kansas 66044



THE UNIVERSITY OF KANSAS / CENTER FOR RESEARCH, INC.

Irving Hill Rd Campus West Lawrence, Kansas 66044

AGRICULTURAL TERRAIN SCATTEROMETER OBSERVATIONS WITH
EMPHASIS ON SOIL MOISTURE VARIATIONS

CRES Technical Report 177-44

C. King

August, 1973

Supported by:
NATIONAL AERONAUTICS AND SPACE ADMINISTRATION
L. B. Johnson Space Center
Houston, Texas 77058
CONTRACT NAS 9-10261



TABLE OF CONTENTS

	<u>Page</u>
ABSTRACT	v
INTRODUCTION	1
BACKGROUND	1
BACKSCATTERING OF MICROWAVES	3
EXPERIMENTAL EQUIPMENTS AND PROCEDURE	11
EXPERIMENTAL RESULTS AND DATA ANALYSIS	13
CONCLUSION	48
REFERENCES	49

LIST OF FIGURES

		<u>Page</u>
Figure 1A	Apparent Relative Dielectric Constant vs. Moisture Content. (Sharkey Clay), (After Lundien)	5
Figure 1B	Conductivity vs. Moisture Content at P-Band. (After Lundien)	6
Figure 2	Relative Dielectric Constant vs. Moisture Content at P-Band. (After Lundien)	7
Figure 3	Complex Dielectric Constant of Corn Leaf Plotted as A Function of Moisture Content. Curves 2-4 Represent Samples Taken From Leaves of the Same Plant. (From Carlson)	8
Figure 4	Average Incoherent Backscattering Cross-Section Per Unit Area With Vertical Polarization. (After Barrick) . . .	9
Figure 5	Radar Signals for Irrigated and Non-Irrigated Fields KU-Band	10
Figure 6A	Drilled Bare Ground with Corn Seeded, KU-Band	14
Figure 6B	Ploughed Bare Ground with Sorghum Seeded, KU-Band . . .	15
Figure 7A	Sorghum 5 Inches, KU-Band	17
Figure 7B	Alfalfa and Sugar Beets, KU-Band	18
Figure 7C	Corn, 19 Inches, KU-Band	19
Figure 8	Average of the Partially Wet and Dry Fields of the Entire Test Site, KU-Band	20
Figure 9A	Average of all the Wet and Dry Fields in the Entire Test Site, KU-Band, Mission 130	21
Figure 9B	Average of all the Wet and Dry Fields in the Entire Test Site, KU-Band, Mission 133	22

LIST OF FIGURES (CONTINUED)

	<u>Page</u>
Figure 10A Distribution of Mean of Agricultural Fields, 10° Incidence.	24
Figure 10B Distribution of Mean of Agricultural Fields, 20° Incidence.	25
Figure 10C Distribution of Mean of Agricultural Fields, 30° Incidence.	26
Figure 10D Distribution of Mean of Agricultural Fields, 40° Incidence.	27
Figure 10E Distribution of Mean of Agricultural Fields, 50° Incidence.	28
Figure 10F Distribution of Mean of Agricultural Fields, 60° Incidence.	29
Figure 11A Distribution of Standard Farm Fields, 10° Incidence.	30
Figure 11B Distribution of Standard Farm Fields, 20° Incidence.	31
Figure 11C Distribution of Standard Farm Fields, 30° Incidence.	32
Figure 11D Distribution of Standard Farm Fields, 40° Incidence.	33
Figure 11E Distribution of Standard Farm Fields, 50° Incidence.	34
Figure 11F Distribution of Standard Farm Fields, 60° Incidence.	35
Figure 12 Backscatter for E-W and N-S Ploughed Bare Fields	37
Figure 13 Backscatter for E-W Planted and N-S Planted Vegetation	38

LIST OF FIGURES (CONTINUED)

	<u>Page</u>
Figure 14A Corn, 36 Inches, P-Band, VV Polarization	39
Figure 14B Corn, 36 Inches, P-Band, HH and HV Polarization	40
Figure 14C Alfalfa and Sugar Beets, P-Band, VV Polarization. . . .	41
Figure 14D Alfalfa and Sugar Beets, P-Band, HH and HV Polarization.	42
Figure 15A Average Backscatter from Mission 130 for 400 MHZ VV Polarization.	43
Figure 15B Average Backscatter from Mission 130 for 400 MHZ HH Polarization.	44
Figure 15C Average Backscatter from Mission 130 for 400 MHZ HV Polarization.	45
Figure 15D Average Backscatter from Mission 133 for 400 MHZ VV Polarization.	46
Figure 15E Average Backscatter from Mission 133 for 400 MHZ HH Polarization.	47

ABSTRACT

Airborne Scatterometer observations were made for agricultural terrain in May and June, 1970 at a NASA test site near Garden City, Kansas. Data from 13.3 GHz and 400 MHz scatterometer were analyzed. It was observed that for incidence angle less than 40° , the 13.3 GHz data showed a difference in backscatter from wet and dry fields of the order of 7 dB. The averages of the various crop types were within a spread of only 5 dB. Other ground parameters such as cultivation pattern and vegetation row effects showed even less distinguishing characteristics on the backscatter. The 400 MHz data also showed a slight moisture dependency.

INTRODUCTION

It is well known that the dielectric constant of a target affects the magnitude of the backscattering of energy incident upon it; and that the moisture content of the target material influences both the real part and the imaginary part of the dielectric constant. Some investigations have been conducted to explore the extent of influence of the moisture variations on the backscattered energy from the ground. It is the purpose of this paper to document the extent of research activities that had been done in the past and to report scatterometer observations of ground moisture variations among changes in other parameters observed at a test site near Garden City, Kansas.

Two scatterometer systems, one operating in the Ku-band and the other in P-band, were used together in the investigations which consisted of two missions flown by NASA/MSR a month apart in the growing season. The Ku-band scatterometer is sensitive to ground moisture changes for antenna viewing angles of 5° - 45° from the vertical whereas the P-band scatterometer shows much less but still observable responses.

BACKGROUND

The moisture content of soil has long been a matter of great concern to hydrologists, agriculturists, environmental conservationists, highway construction engineers, farmers, etc. Accurate determination of the amount of the moisture content in the soil can be accomplished by measurement in the field which is time consuming and, in many cases, impractical. Therefore a need exists to measure soil moisture content by remote sensing devices.

The earliest and still the most widely employed remote sensing tool is photography. Aerial photo reconnaissance is useful in a limited capacity to infer the gross top soil moisture condition by nature of its tonal contrast¹. Its satisfactory operation is heavily dependent upon favorable weather condition and the presence of adequate ambient light.

Photographic sensors that operate in the infrared spectrum are also inadequate because they are only sensitive to the surface soil of a fraction of a millimeter. Sub-surface moisture variations, which could be indicative of the presence of two types of soil of different porosity and permeability, would not be detected by such sensors.

Electromagnetic radiation at microwave frequencies has been utilized to assess the moisture status of soil. Edgerton's studies^{2, 3} with microwave radiometers showed that measured microwave temperature is dependent on sensor frequency and polarization, and that sizable differences in radiometric response are caused by differences in moisture content, particle size, and surface roughness. Particle size and surface roughness variations influence the general shape and slope of the radiometric temperature vs antenna viewing angle plots whereas moisture content variations cause the curve to shift along the temperature axis. MacDonald and Waite⁴ also reported a delineation of soil moisture difference on side-looking airborne radar imagery. Here again, the same factors, i.e. surface roughness, incidence angle, polarization, frequency, dielectric properties, etc, govern the backscatter radiation pattern. It is well known that moisture content variations in the radar target will change its dielectric properties and different amount of microwave energy is backscattered when the dielectric properties of the scatterer change.⁵

Of all the sensors mentioned above, the side-looking radar seems to be the most promising instrument for ground moisture detection. Unlike photographic sensors that operate in the visible range of the spectrum, microwave imagers are operational under diverse weather conditions. Since the imager is an active sensor, the lack of ambient light does not hamper its operation. Furthermore, the returned signal does not come from the surface alone, as in the case of visible and infrared sensors, but from the upper volume of the soil as well. Therefore, subsurface moisture variations can also be monitored. The advantage of sidelooking radar over the other sensors that operate in the microwave region, such as radiometers and scatterometers, becomes more apparent as the sensor platform increases from aircraft to space satellite altitude. With radiometers and scatterometers, degraded resolution parallel with increasing range, whereas with the advent of synthetic aperture, fixed resolution independent of range is possible with the fully focused synthetic aperture imager.

In spite of its advantages over the other sensors, actual field data from imaging radar on soil moisture variation is scarce. One of the reasons could be that the majority of present imaging radars scan from 40° incidence outward to near grazing while it has been reported⁶ that to detect gross soil moisture changes, the incidence angles have to be less than 45°.

Airborne scatterometer systems, such as the NASA 13.3 GHz vertically polarized and the 400 MHz multi-polarized scatterometers, allow for more detailed observation of radar scattering behavior than radar imagers⁷. Variations of scattering coefficients with incidence angles can be observed with scatterometry. With some scatterometer systems, the effect of polarization and wavelength can also be studied. The trade-off for these added features comes in poorer resolution and less ground coverage. In order to determine the optimum parameters such as dynamic range, incidence angle, frequency, polarization, etc., for the design of a specific imaging radar, the terrain scatterometry data analysis becomes especially helpful. The description of an operational system and its data analysis showing the effect of soil moisture as well as other ground parameters will be discussed later in the report.

BACKSCATTERING OF MICROWAVES

The backscattered radiation is affected by both the sensor parameters and the ground parameters. For a radar imager, the sensor parameters are viewing angles, polarization, wavelength, power, and illuminated area. The ground parameters include the complex dielectric properties, surface roughness, subsurface roughness to depth where attenuation reduces waves to negligible amplitudes⁸, and possible layering effects.⁹

Although theories have been formulated and many controlled programs conducted, the scattering problem under field conditions has not been solved. It is known, in general, that surfaces with RMS roughness heights much less than the order of a wavelength are smooth, and scattered energy is strongest in the specular direction. On the other hand, surfaces with the roughness on the order of a wavelength or more are rough and scattered energy tend to be more isotropic.¹⁰

The complex dielectric properties affect the returned energy in a different manner. For a given rough surface at a fixed viewing angle, the higher the complex dielectric constant, the greater will be the amount of returned energy.

The effect of changes in the moisture content is known to change the dielectric properties of the backscatterer. Lundien⁵ conducted a carefully controlled experiment at the U. S. Army Engineer Waterways Experimental Station to determine

the radar response to laboratory prepared soil samples. The soil samples were placed in a cart and the top surface smoothed over. The cart was then placed at the axis of a large arch along which multi-frequency radars could gather the radar response of the soil under test for different viewing angles. The most important finding in this effort is a documentation of the variations in dielectric properties of the soil samples as a function of the moisture content (Figure 1 a-b). Lundien also indicated that the dielectric constant of soil depends only on the quantity of water, and the effect of soil type is minor at P-band (Figure 2). A similar experiment dealing with plant moisture content was done by Carlson¹¹ at Ohio State University. Figure 3 shows some of the results of Carlson's investigations.

Barrick and Peake¹² did theoretical investigation in backscatter from slightly rough surfaces using the perturbation approach. Figure 5 cites one of their results. In this figure, a Gaussian correlation function was used to model the spatial auto-correlation function of surface heights. Although such functions are mathematically tractable, they fail to agree with other experimental curves for incidence angles away from the vertical.⁸ Nevertheless, it serves to illustrate the vertical displacement of the radar cross section curve as the dielectric constant changes.

In the sections following, radar return from very wet vegetated land ($\epsilon/\epsilon_0 \approx 30$ or higher) will be compared with that from the dry vegetated land ($\epsilon/\epsilon_0 < 10$). This is done by selecting fields where irrigation was in progress at the time of the mission. Parts of the field where irrigation water had flowed in would constitute the wet land while the unirrigated portion would be the dry land. The moisture dependency will then be compared with other ground parameters. These analyses will follow after a discussion on the experimental procedures and equipments used.

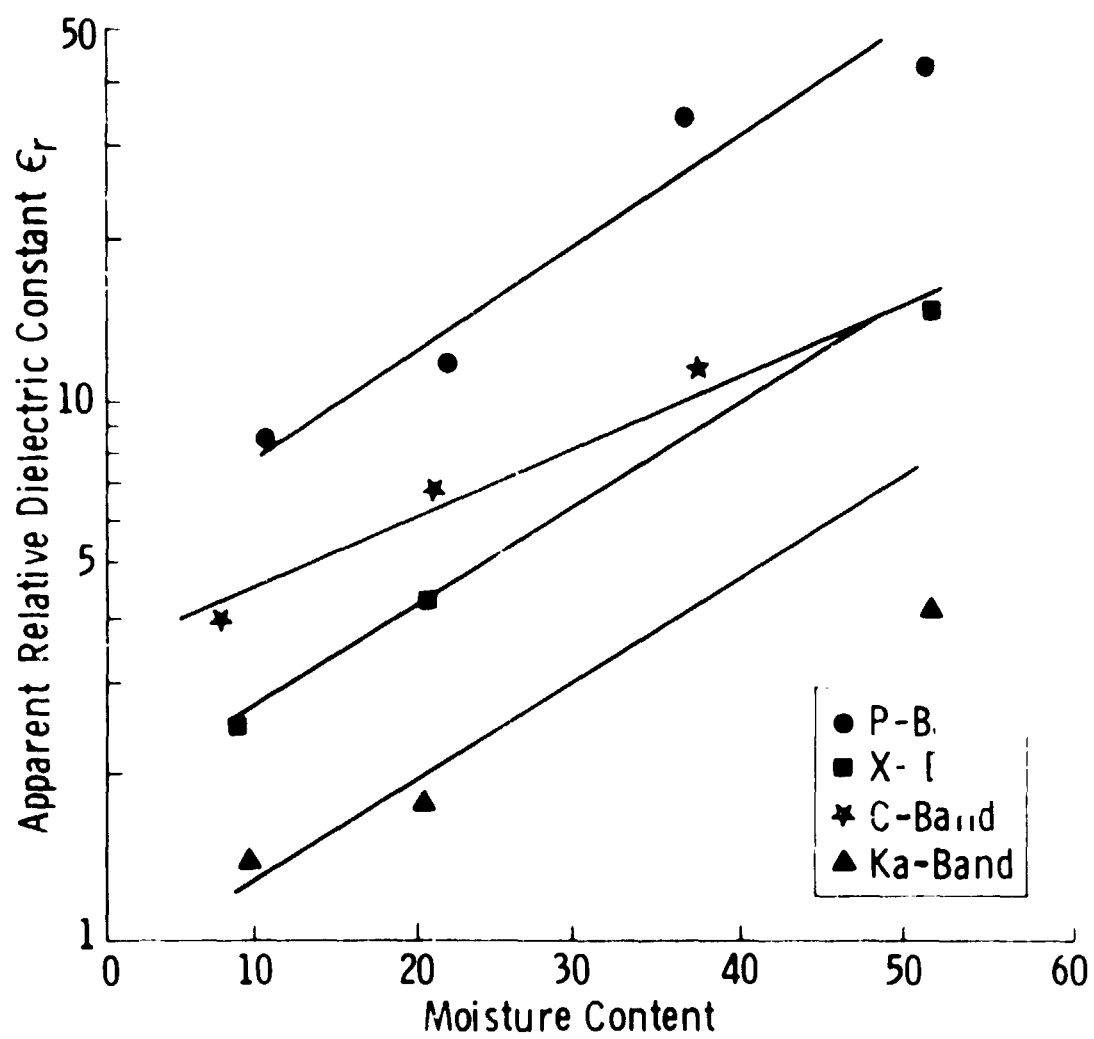


FIGURE 1A. APPARENT RELATIVE DIELECTRIC CONSTANT VS. MOISTURE CONTENT. (SHARKEY CLAY), (AFTER LUNDIEN)

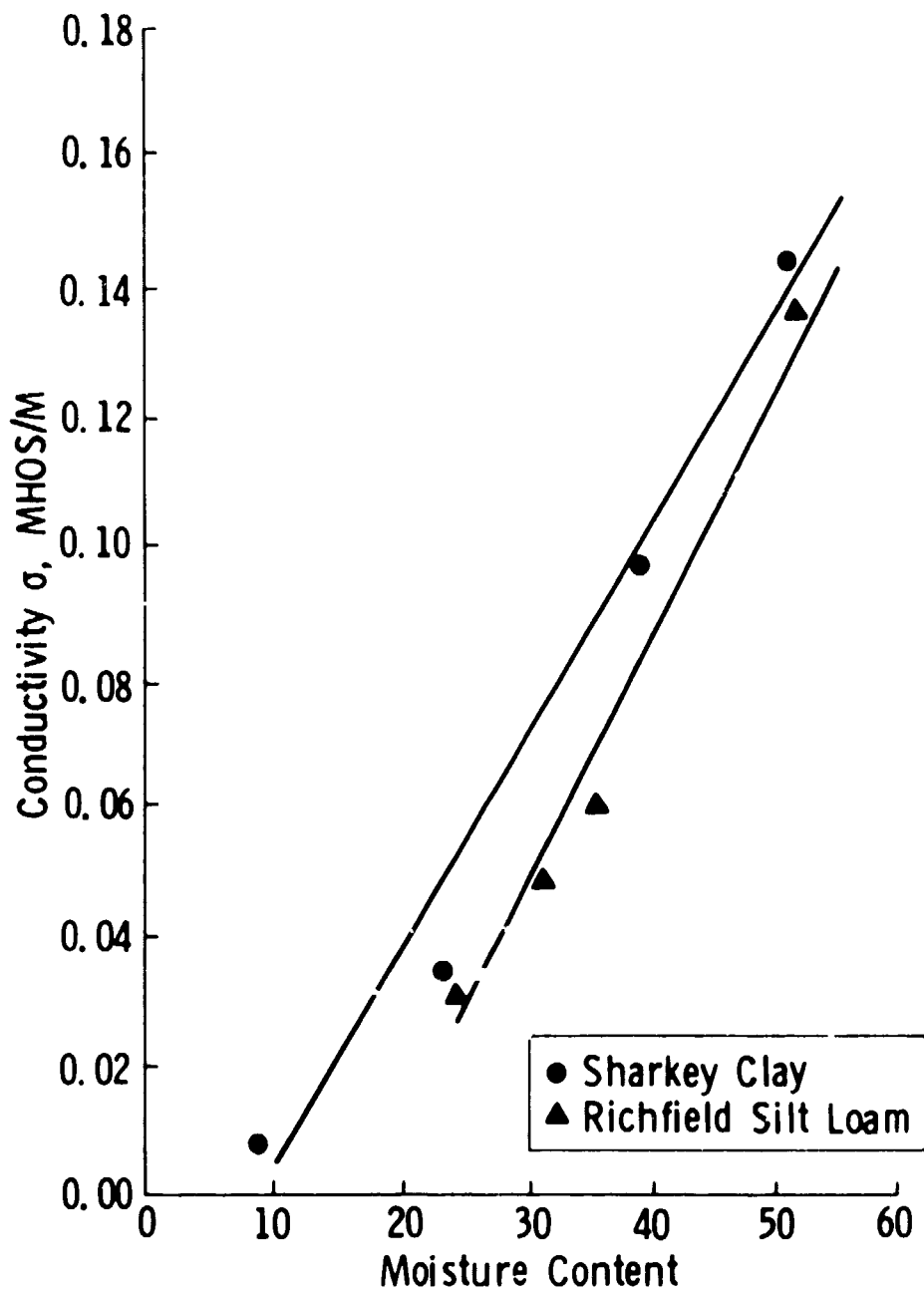


FIGURE 1B. CONDUCTIVITY VS. MOISTURE CONTENT AT P-BAND.
(AFTER LUNDIEN)

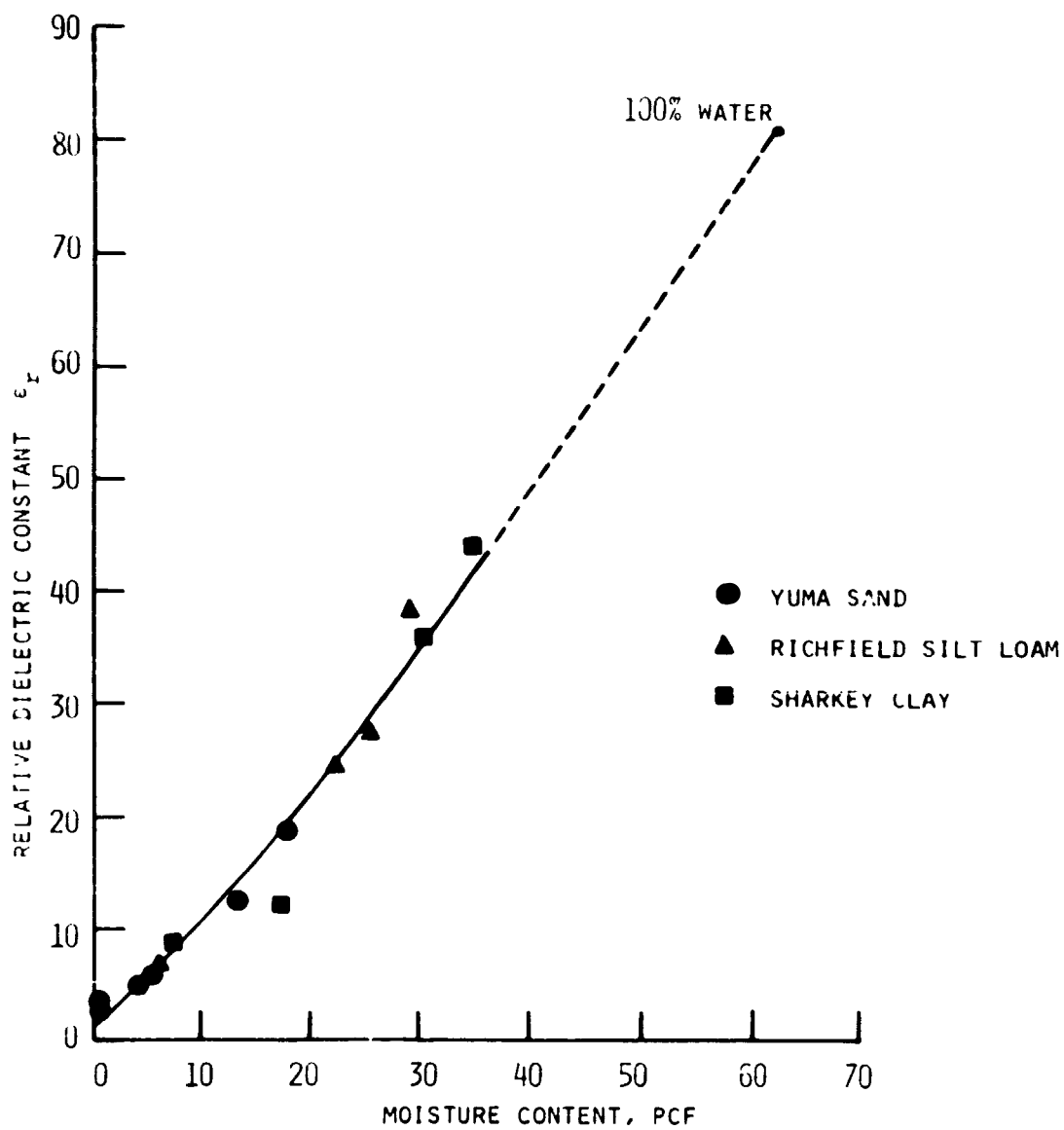


FIGURE 2. RELATIVE DIELECTRIC CONSTANT VS. MOISTURE CONTENT AT P-BAND. (AFTER LUNDIEN)

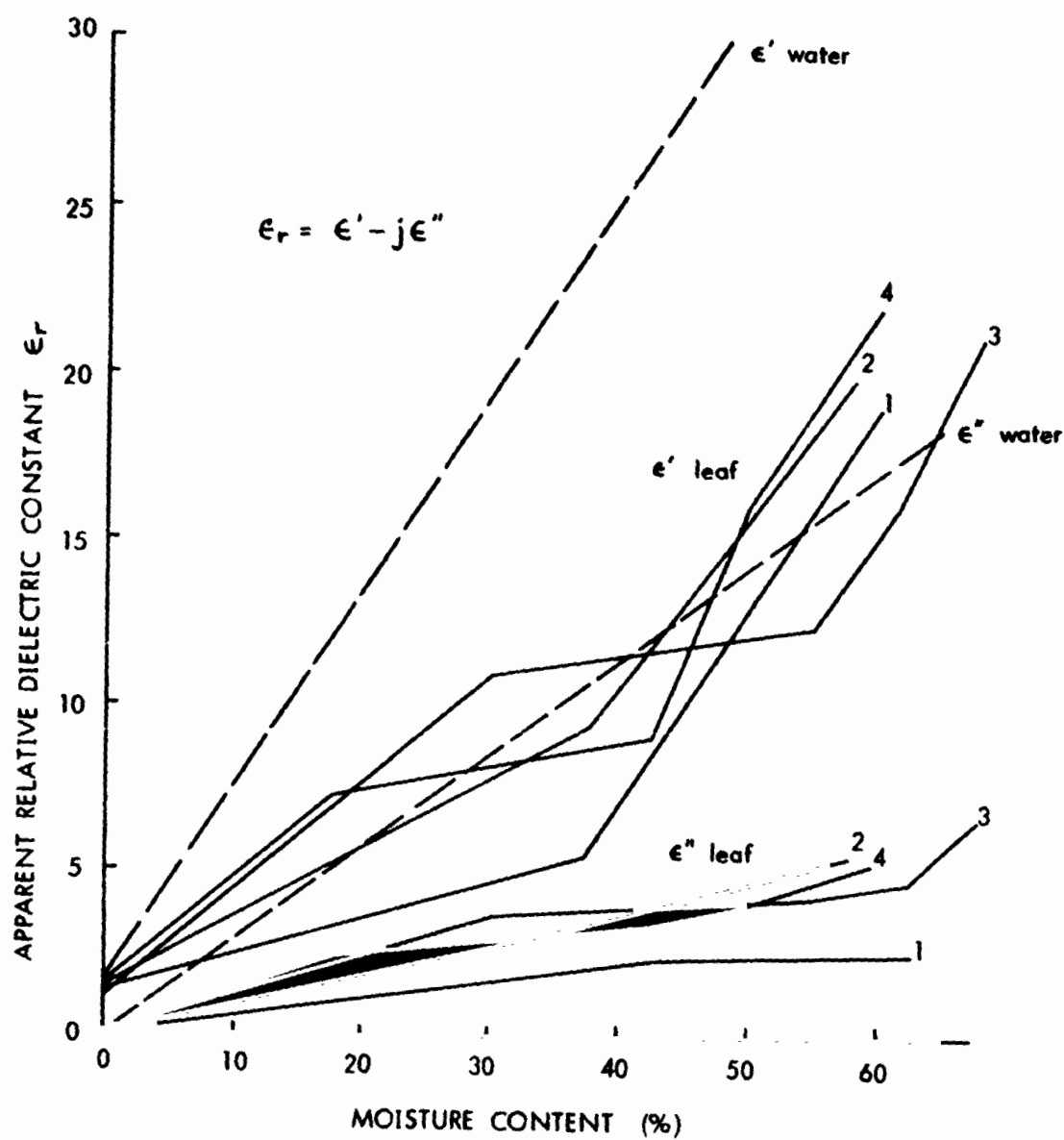


FIGURE 3. COMPLEX DIELECTRIC CONSTANT OF CORN LEAF PLOTTED AS A FUNCTION OF MOISTURE CONTENT. CURVES 2-4 REPRESENT SAMPLES TAKEN FROM LEAVES OF THE SAME PLANT. (FROM CARLSON)

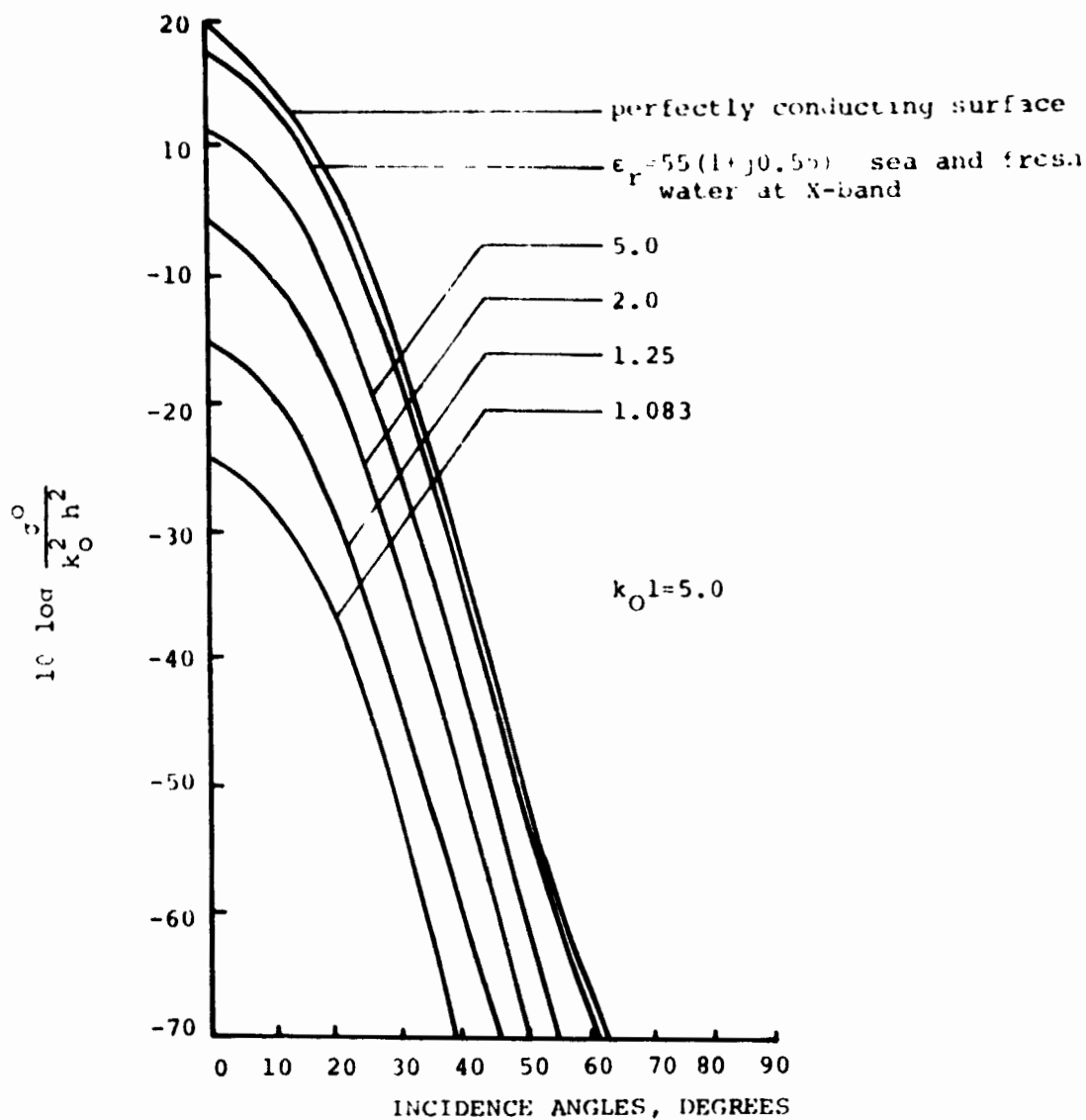


FIGURE 4. AVERAGE INCOHERENT BACKSCATTERING CROSS-SECTION PER UNIT AREA WITH VERTICAL POLARIZATION. (AFTER BARRICK)

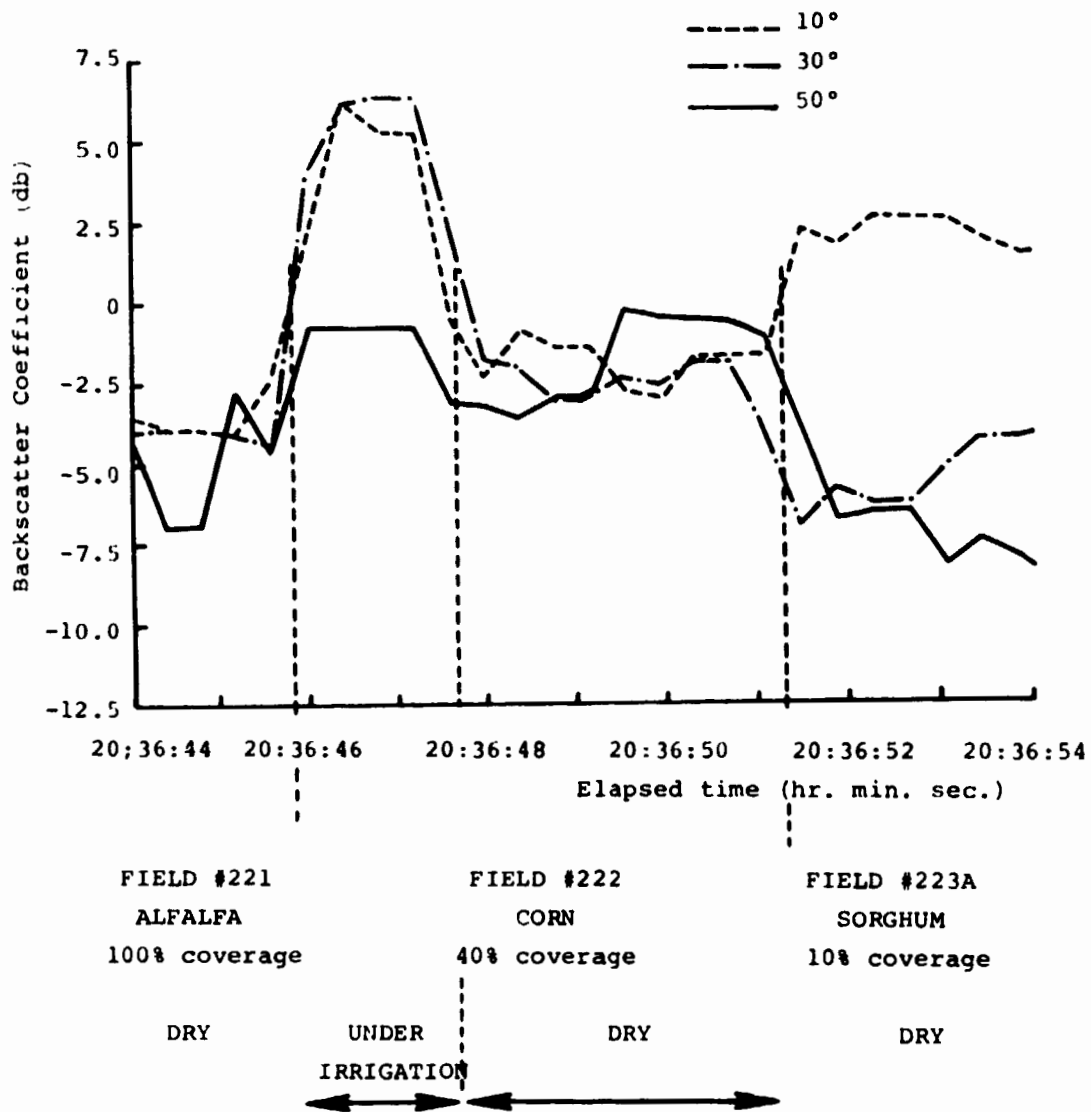


FIGURE 5. RADAR SIGNALS FOR IRRIGATED AND NON-IRRIGATED FIELDS, KU-BAND.

EXPERIMENTAL EQUIPMENTS AND PROCEDURE

The data analyzed in this report were obtained during the two missions made on 27 May and 26 June, 1970 from NASA/JSC using 0.4 and 13.3 GHz scatterometers. Both missions were conducted over the same test site, 76, near Garden City, Kansas.

Both radar scatterometers were carried in a P3A aircraft, with antennas mounted beneath the wing and fuselage (0.4 GHz) and on the bottom of the fuselage (13.3 GHz). Antenna patterns are fan shaped, with narrow beams transverse to the flight path, and wide beams along the flight path. Angle of incidence within the wide beam is determined by filtering out appropriate Doppler-shifted components of the return. The 0.4 GHz system uses a superheterodyne receiver to process the backscatter and a calibrated signal located 500 Hz above the transmitted frequency. The end result is a translated replica of the Doppler spectrum about the center line of the transmitted spectrum plus the calibrated signal 500 Hz above the zero Doppler point.¹³ By knowing aircraft velocity and transmitted frequency, it is possible to make a translation between Doppler frequency and angle. The 13.3 GHz system uses a homodyne receiver with in-phase and quadrature channels to permit recording components necessary to separate the positive and negative Doppler shifts in the analysis. The 13.3 GHz antenna has a cross-track beam width of 2.5° and is only vertically polarized. The 0.4 GHz antenna has a cross-track beam width of 6.7° and has both vertically and horizontally polarized elements. Thus it can be used to obtain four polarizations: VV, HH, VH, and HV.

As the aircraft flies by a patch of ground, the first signal observed is from a point 60° ahead of vertical; later the signals from this patch are received at other angles down to vertical itself, and then as the aircraft flies away the incidence angles from this patch again increases out to 60° . The ground returns from the different angles are therefore displaced from each other in time, with the $+60^\circ$ signal arriving first and the -60° signal last. These displacements are removed in data processing so that observations from a given point on the ground may be observed simultaneously for the different angles.

The Garden City test site consists of an area of 600 fields about three miles north-west of Garden City, Kansas. In this region the terrain is very flat, and both irrigated and dryland farming are practiced. Crops grown include alfalfa, corn, grain sorghum, sugar beets, wheat, and hay. The fields are large and laid

out in a rectangular grid bounded on the east and west by parallel roads a mile apart. Many of the fields are half a mile wide, but another large group is only a quarter mile wide. The flight path of the mission aircraft was parallel to the north-south road and a quarter mile from the road, so that it passed through the center of the half mile wide fields but along the boundaries of the quarter mile wide fields. At the flight altitude of 3000 feet, the half power illuminated width of the 13.3 GHz scatterometer is 131 feet and the 0.4 GHz system is 320 feet. Actually this beam width is somewhat different at different angles of incidence, for the beam is not a perfect fan, but the values used may be considered representative.

Aerial photographs were obtained during the scatterometer run, so that the path of the aircraft can be plotted by mosaicking these pictures. Hence, the locations of the illuminated areas are well established. Ground parties visited all the fields along the road, although some of the fields away from the road were missed; air-photo interpretation permits reasonable estimates to be made of the state of these fields in terms of the information gathered for similar looking fields. The ground parties recorded the following information: vegetation type, percent ground cover, heights of plants, growth stage, crop condition, clod size, cracking and crack size, salt accumulation, ground treatment, row directions, qualitative moisture description, type of irrigation, and ground photos. For some fields, information was collected on plant moisture content at various levels (determined by bringing samples to the lab for weighing and drying). For a few fields, soil moisture content was determined with a neutron probe. Unfortunately the soil moisture was not measured in the fields being irrigated at the flight time.

Data processing by NASA/JSC involves converting recorded signal spectra into values of scattering coefficient for each ground element and angles. The results are plotted both as σ^0 vs. time with angles as a parameter and as graphs of σ^0 vs. angle for each ground element. The time plots are aligned with the photo mosaics to allow grouping of the ground elements associated with each field. Ground elements are observed long enough to obtain moderately good averages of the fading signals, although a compromise is necessary because of the inconsistency of good averaging and good resolution.¹⁴ For 13.3 GHz each element represents 150 feet along the track and for 0.4 GHz it is 450 feet. For this observation involving partial fields, the 450 foot cells probably were too long, and reprocessing of the data may be necessary to allow adequate resolution of the field segments.

EXPERIMENTAL RESULTS AND DATA ANALYSIS

In both missions, the same aircraft, NASA 927-NP3A, was used for in-flight data gathering. This eliminated the problems caused by different aircraft structures on the antenna beam. The following analysis involves the entire data set for mission 133 and the first half of the bulk of data from mission 130. This is due to the fact that the time history data from the last three runs of mission 130 were abnormally flat (less than 5 db dynamic range) compared to a normal dynamic range of 13-18 db for agricultural terrain. Since the test site was fairly homogeneous as evidenced from aerial photo mosaics, the discontinuity between the first three flight lines and the remaining three lines was attributed to sensor system malfunction and the associated data from the last three lines was not used.

The scatterometry data originally obtained from NASA/JSC were in two forms: the scattering coefficient time history for different angles with time as a variable, and the scattering coefficient vs. antenna viewing angle plots for each resolution cell on the ground. In aligning the scatterometry time history with the simultaneously obtained aerial photography, it was found that a sharp increase in backscatter on the order of 5-7 db, with incidence angles less than 40° , was observed for agricultural fields under irrigation (Figure 5). For mission 130, flown by NASA on June 26, 1970, it was found that at the time of overflight eleven fields were being irrigated completely and eight fields were partially being irrigated. As for mission 130, conducted on May 27, 1970, there were five totally irrigated and two partially irrigated fields. Table 1 lists the ten partially wet fields from both missions together with their respective crop types, crop height, and percent ground cover.

The analysis of these partially wet and partially dry fields will illustrate the effect of changing the dielectric properties of the ground scatterers. This is valid because the only variable within each field is the moisture content of the soil.

Looking at the data from mission 130, only two partially irrigated fields were included. They were both bare fields where one was plowed and the other drilled. At 13.3 GHz the scattering coefficient, σ° , curves for the wet and dry segments for both fields are plotted in Figure 6 a-b. The wet σ° curves, in both cases, were above the dry curves by about 5 db or more for incidence angles less than 35° from the vertical. It is interesting to note that while both fields are

MISSION 130

SITE GARDEN CITY, KANSAS

FREQUENCY 13.3GHz

DATE MAY 27, 1970

POLARIZATION VV

FIELD 159

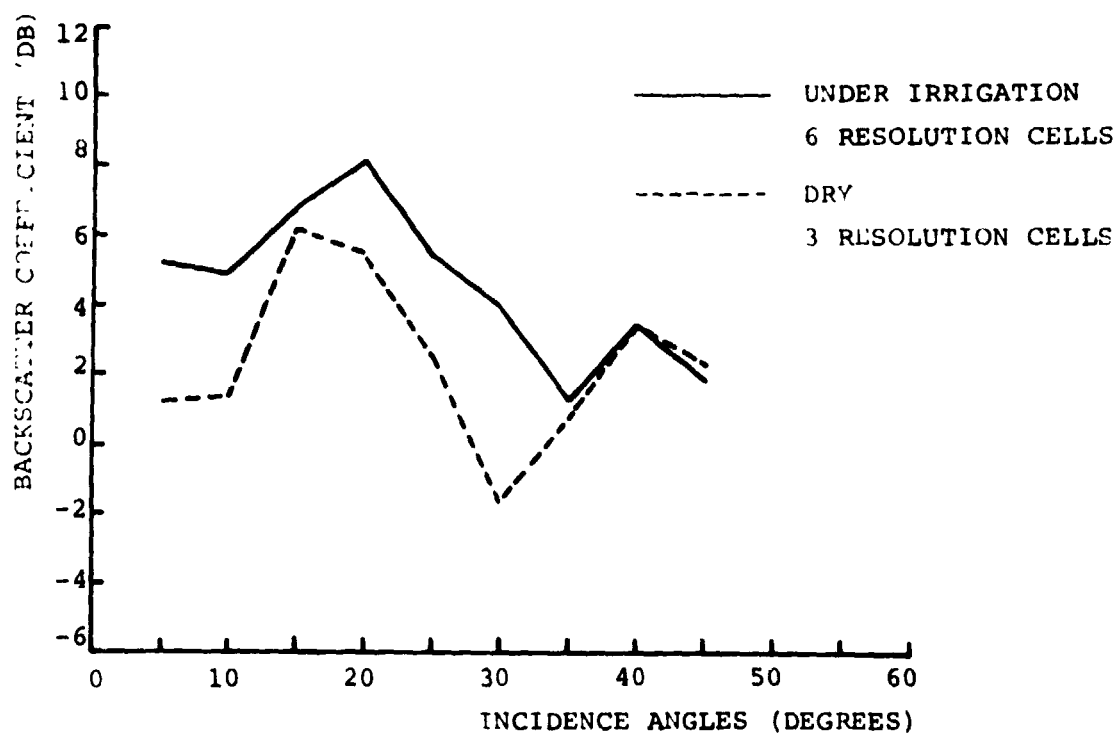


FIGURE 6A. DRILLED BARE GROUND WITH CORN SEED, KU-BAND.

MISSION 130

SITE GARDEN CITY, KANSAS

FREQUENCY 13.3 GHz

DATE MAY 27, 1970

POLARIZATION VV

FIELD 139

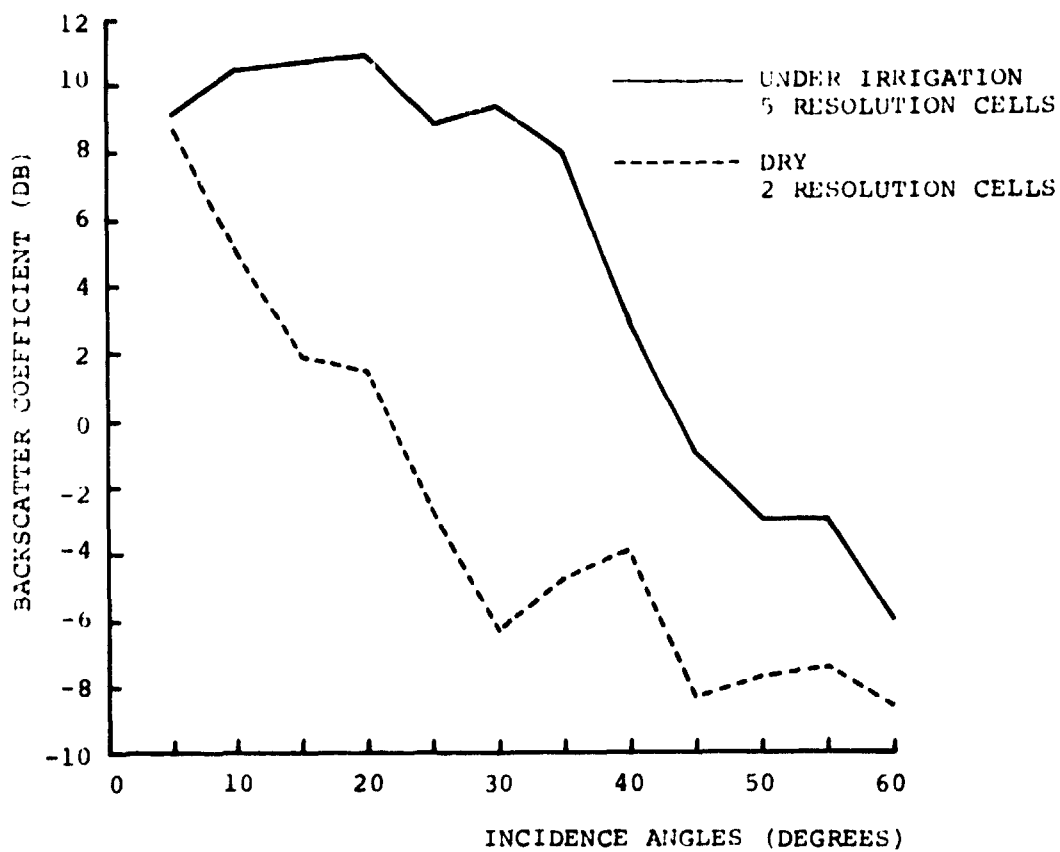


FIGURE 6B. PLOUGHED BARE GROUND WITH SORGHUM SEED, KU-BAND.

TABLE 1.
PARTLY IRRIGATED AND PARTLY DRY FIELDS

<u>Mission</u>	<u>Field #</u>	<u>Crop Type</u>	<u>Crop Height</u>	<u>Vegetation Coverage</u>
130	139	plowed bare ground	NA	0%
130	159	drilled bare ground	NA	0%
133	27	corn	36"	70%
133	108A	alfalfa & sugar beets	NA	NA
133	119A	corn & bare ground	NA	NA
133	222	corn	19"	40%
133	229	corn	7"	10%
133	412	sorghum	5"	5%
133	425	alfalfa	10"	100%
133	435	alfalfa	13"	100%

bare, the slopes of the σ^0 curves are quite different. The plowed field, having distinctive rows and large clods (2-3" diameter), bear the resemblance of a composite surface; and the drilled field, having no rows and very fine clods, might be approximated by the small perturbation surface.¹⁵ On the other hand the eight partially irrigated fields from mission 133 were all vegetated fields. Using the same approach, the σ^0 curves of the wet and dry segments are plotted on the same graph for each of the eight fields. Figure 7 a-c are three samples of these graphs. Although the shapes of the σ^0 curves in Figure 7 have the added contribution from different crop types besides the original effects from rows and clods, the general trend is still a separation of about 7 db from the change in ground moisture for incidence angles less than 40°. Above 40° the two curves tend to converge.

This trend is best exhibited in Figure 8, which is an average of the eight partially irrigated fields of mission 133. As a further check on the trend, averaged σ^0 curves were computed for all the fields in the test site that might be considered dry and all fields that might be considered wet. These curves are shown in Figure 9 a-b. Figure 9a is an average of eight wet fields and forty-five dry fields from mission 130, and Figure 9b is an average of nineteen wet fields and 687 dry fields from mission 133.

MISSION 133

SITE GARDEN CITY, KANSAS

FREQUENCY 13.3 GHz

DATE JUNE 26, 1970

POLARIZATION VV

FIELD 412

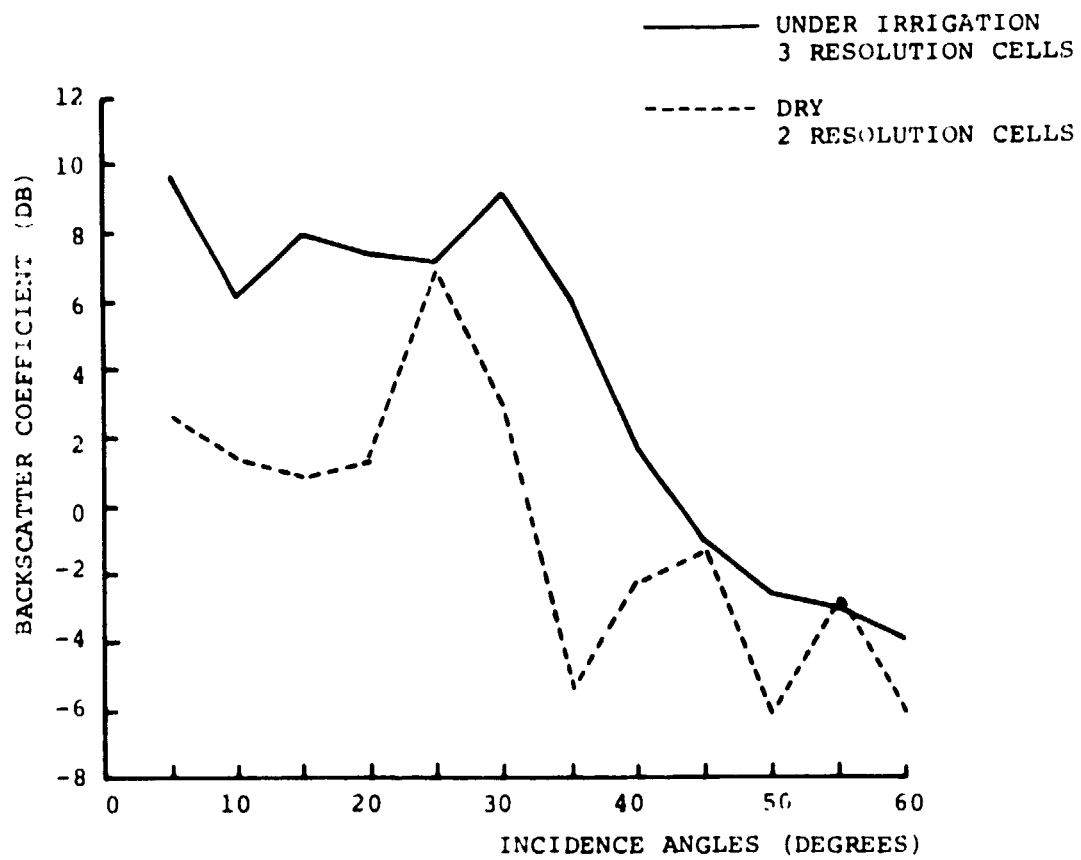


FIGURE 7A. SORGHUM 5 INCHES, KU-BAND.

MISSION 133

SITE GARDEN CITY, KANSAS

FREQUENCY 13.3 GHz

DATE JUNE 26, 1970

POLARIZATION VV

FIELD 108

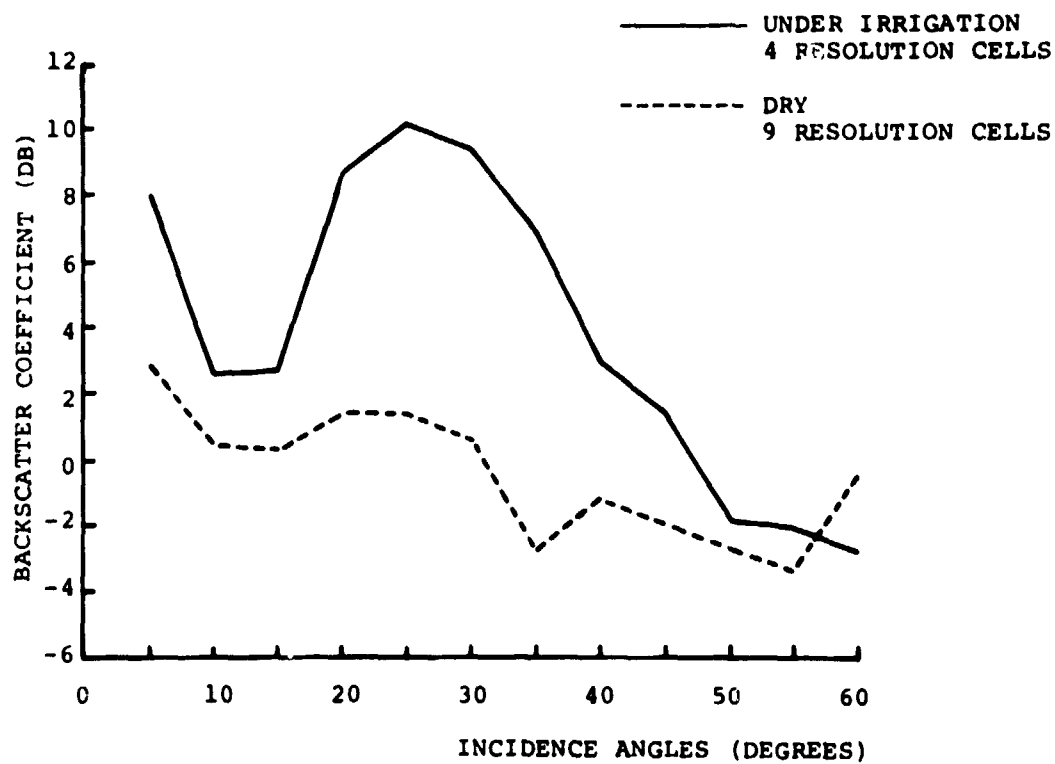


FIGURE 7B. ALFALFA AND SUGAR BEETS, KU-BAND.

MISSION 133

SITE GARDEN CITY, KANSAS

FREQUENCY 13.3 GHz

DATE JUNE 26, 1970

POLARIZATION VV

FIELD 222

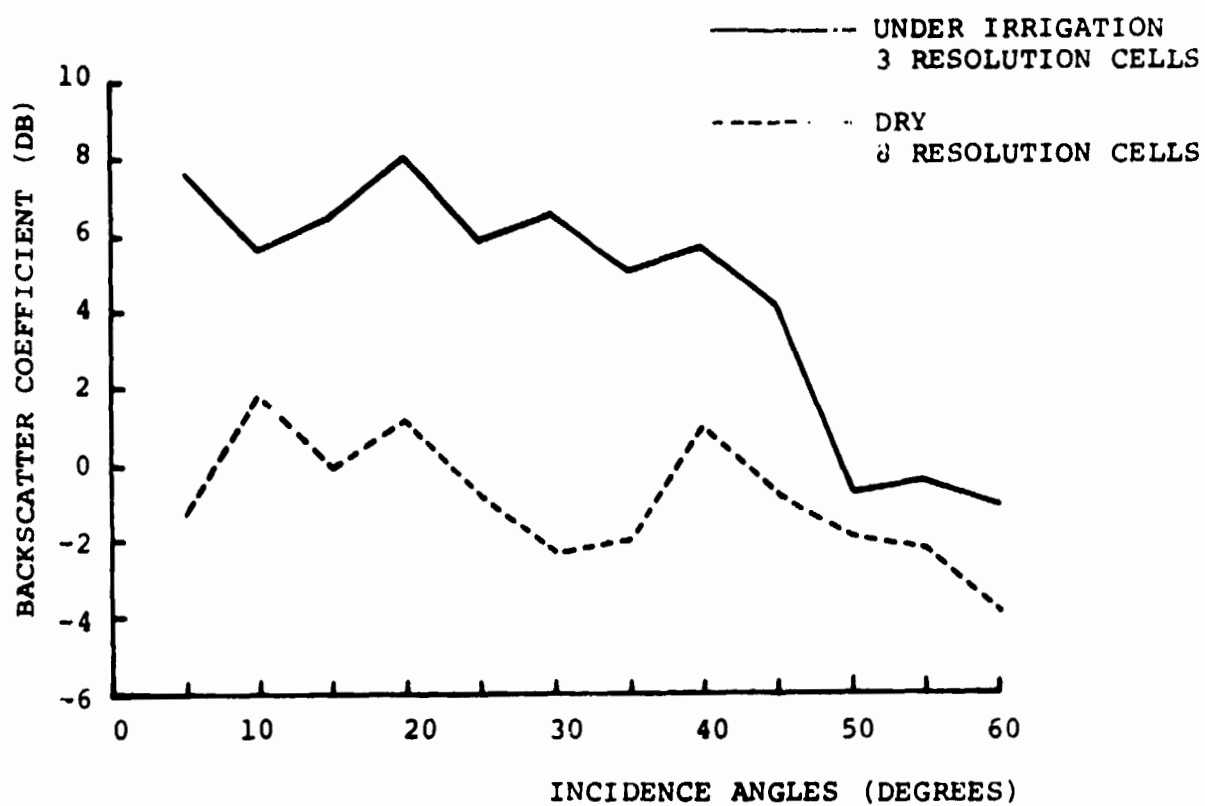


FIGURE 7C. CORN, 19 INCHES, KU-BAND.

MISSION 133

SITE GARDEN CITY, KANSAS

FREQUENCY 13.3 GHz

DATE JUNE 26, 1970

POLARIZATION VV

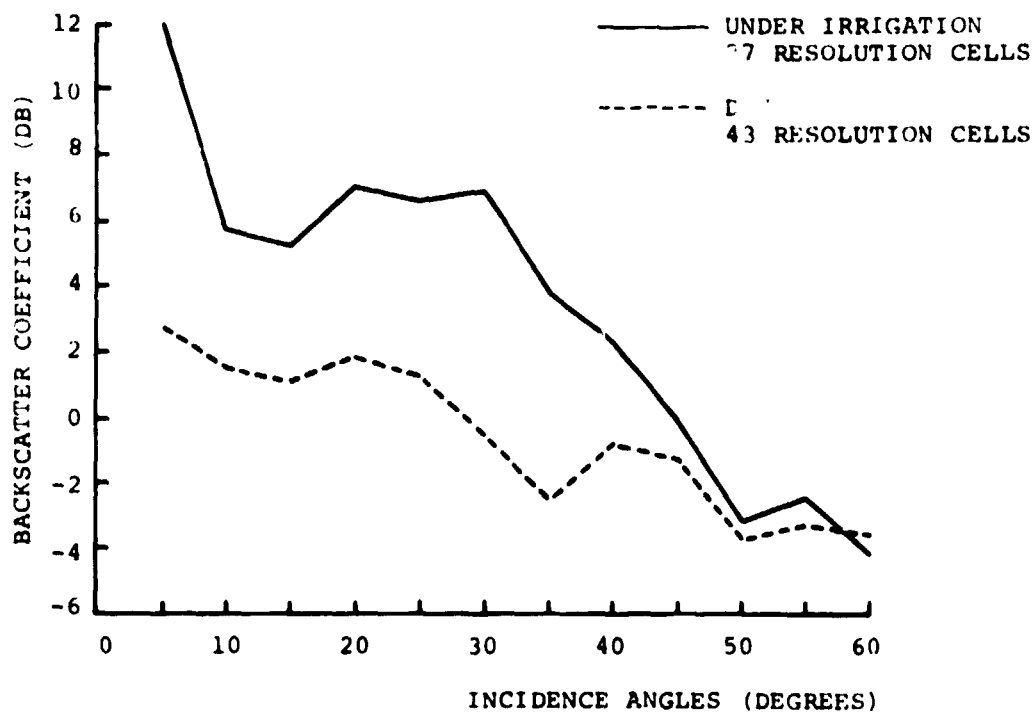


FIGURE 8. AVERAGE OF THE PARTIALLY WET AND DRY FIELDS OF THE ENTIRE TEST SITE, KU-BAND.

MISSION 130

SITE GARDEN CITY, KANSAS

FREQUENCY 13.3 GHz

DATE MAY 27, 1970

POLARIZATION VV

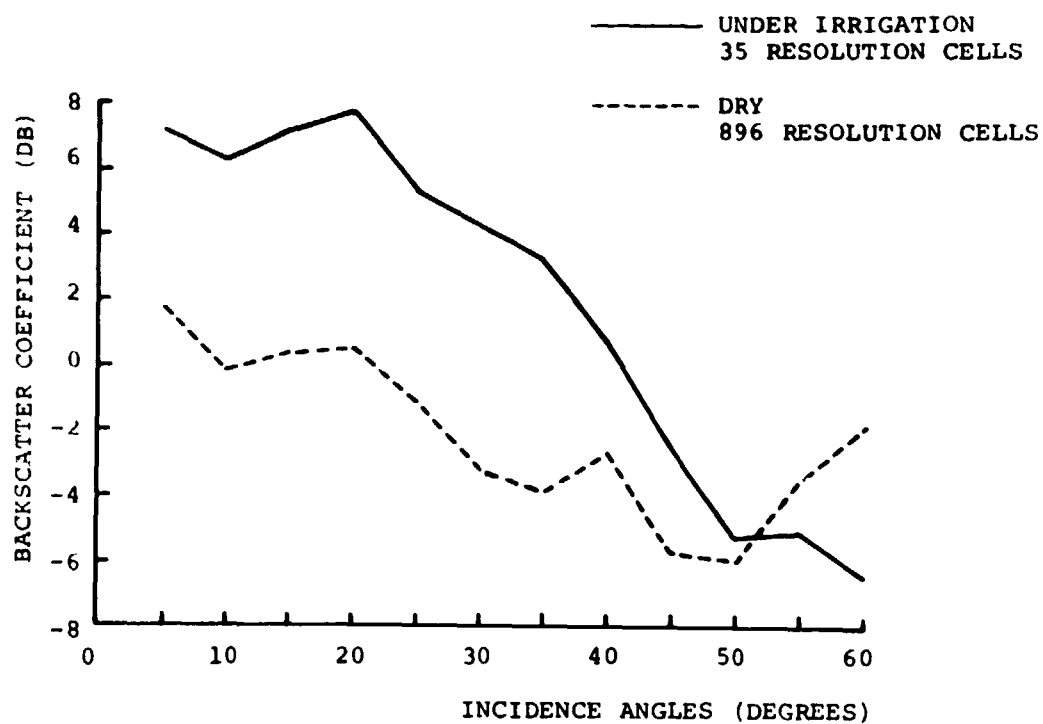


FIGURE 9A. AVERAGE OF ALL THE WET AND DRY FIELDS IN THE ENTIRE TEST SITE, KU-BAND, MISSION 130.

MISSION 133

SITE GARDEN CITY, KANSAS

FREQUENCY 13.3 GHz

DATE JUNE 26, 1970

POLARIZATION VV

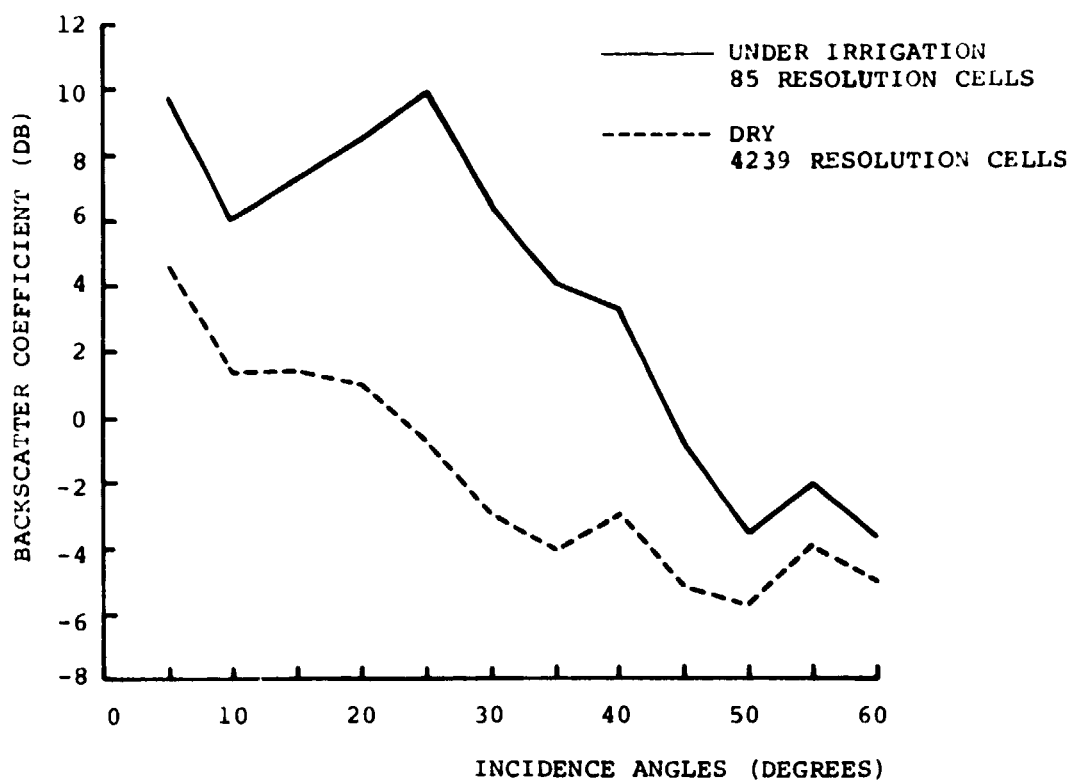


FIGURE 9B. AVERAGE OF ALL THE WET AND DRY FIELDS IN THE ENTIRE TEST SITE, KU-BAND, MISSION 133.

It is interesting at this point to examine the differences in backscatter from various crop types and compare with the variation within the same field due to moisture difference. The data from mission 133 was categorized according to crop type for each of the antenna viewing angles. The mean of each field in the test site is computed and a plot is made for the spread of all the means of the individual fields at a particular incidence angle. For each crop type, the average of the fields belonging to that crop was calculated. Figure 10a-10f are histograms showing the absolute return of the fields in the test site at various incidence angles. The irrigated fields were not included in the plots. Each dot represents the mean value of a field, and the bar is the average of all the fields that fall within a particular crop category. The shaded regions represents the spread of one standard deviation from the mean.

It can be seen from the histograms that a hint of clustering can be made among the crops considered, especially at 30° and 40° incidence. The usually irrigated crops of corn, sorghum, and sugar beets exhibited higher returns than the much drier wheat stubbles, weeds, and grain wheat which were mostly ripe and dry in the month of June. The categories of alfalfa and bareground fell somewhere in between.

It is also observed that the averages of all the categories of crops considered fall within a spread of only 5 dB, and the overlapping of the means of the individual fields belonging to different categories on the vertical axis is significant. For other viewing angles, the overlapping is even more pronounced.

In an attempt to further segregate the different crop types, the technique known as the Standard Farm approach is applied. In the Standard Farm approach, only fields having homogeneous, healthy crops of at least 30 per cent ground coverage were enlisted. For example, alfalfa fields of the Standard Farm quality would be in full bloom, and bare fields were tilled, ploughed, or cultivated fields free of stubble or stalks. Figures 11a-11f are the distribution of the Standard Farm Fields. Notice that categories such as sorghum and sugar beets have been deleted since they have not attained sufficient growth in the month of June, and the category "weeds" was composed of an assortment of weeds and hence not considered.

With the Standard Farm Fields, the distinctions among crops are enhanced. Thirty degrees and 40° incidence angles are still the optimal angles for crop separation and it can be seen that corn is almost completely differentiable at 30° , and at 40° the lowest return is dominated by standing wheat stubble and the dry and ripe wheat.

Mission 133 June 26, 1970
 Frequency : 13.3 GHz
 Polarization : HH
 $\theta : 10^\circ$ Incidence

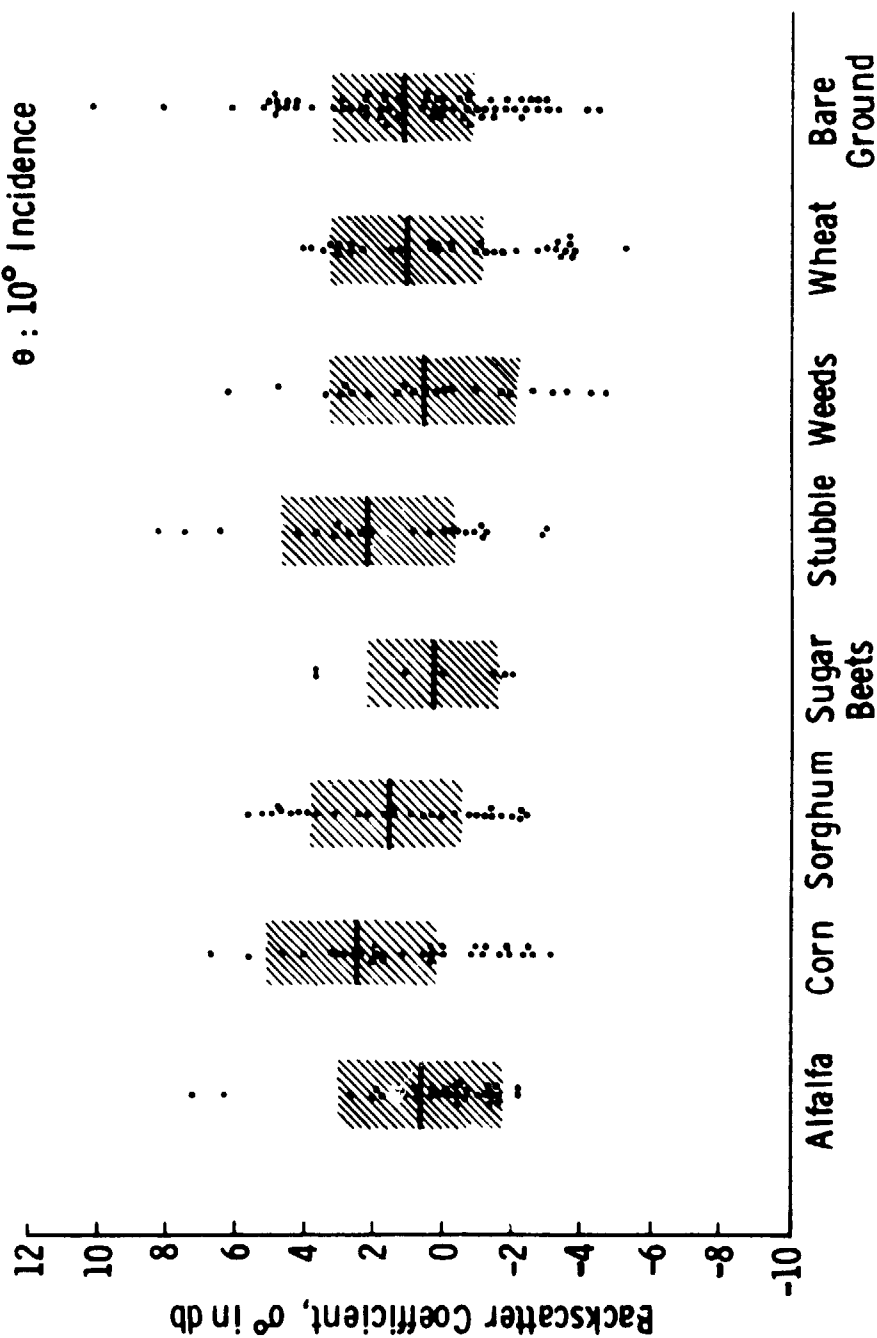


FIGURE 10A. DISTRIBUTION OF MEAN OF AGRICULTURAL FIELDS,
 10° INCIDENCE.

Mission 133 June 26, 1970
 Frequency : 13.3 GHz
 Polarization : VV
 θ : 20° Incidence

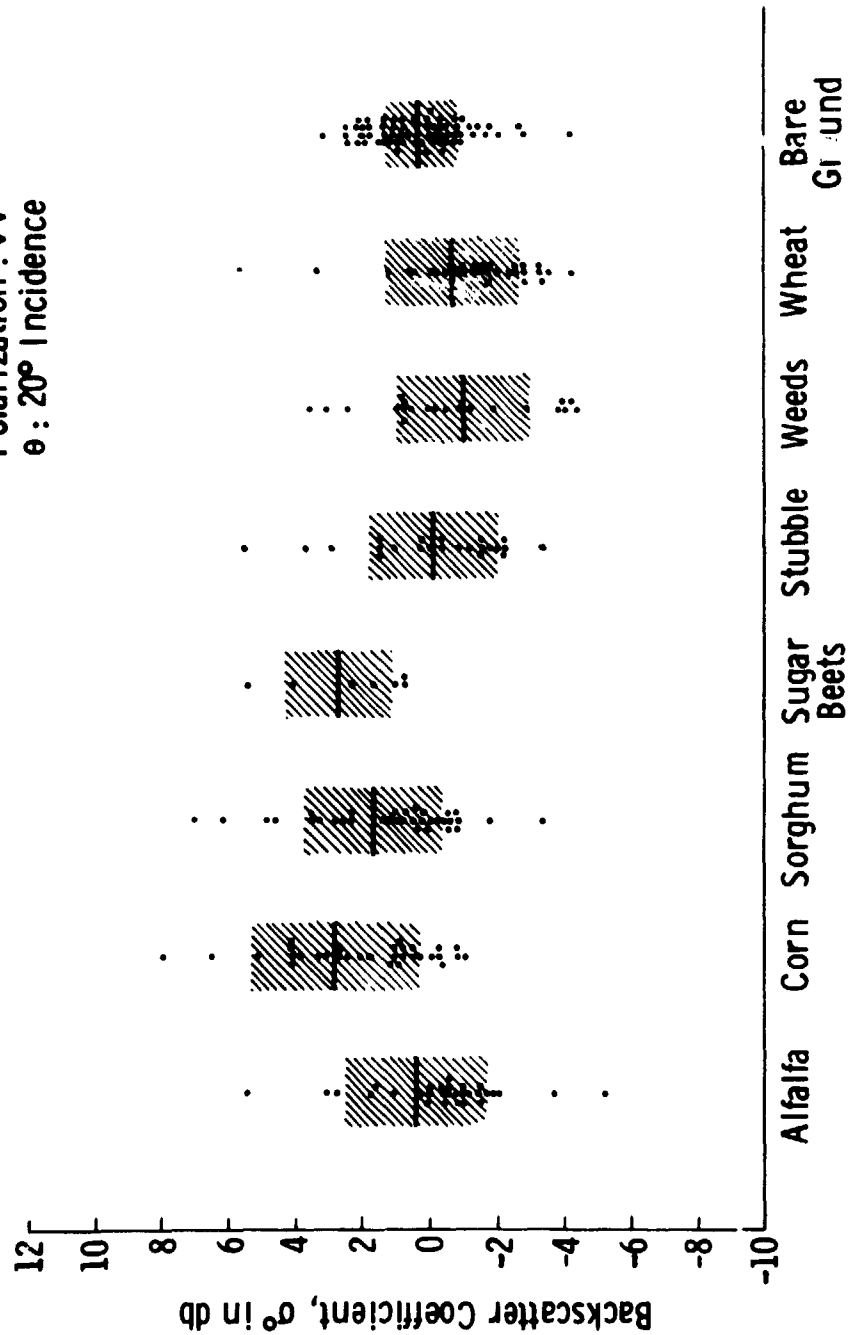


FIGURE 10B. DISTRIBUTION OF MEAN OF AGRICULTURAL FIELDS, 20° INCIDENCE.

Mission 133 June 26, 1970
 Frequency : 13.3 GHz
 Polarization : VV
 θ : 30° Incidence

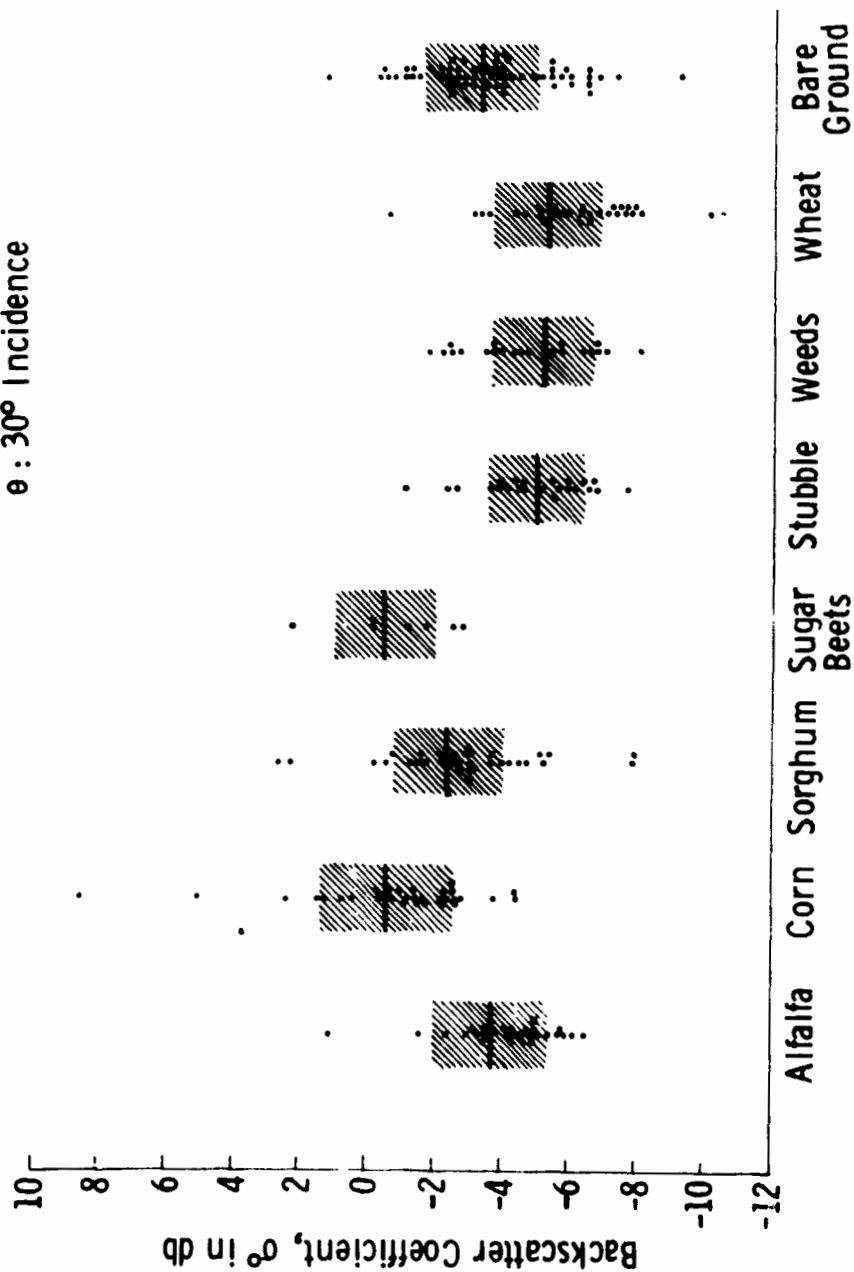


FIGURE 10C. DISTRIBUTION OF MEAN OF AGRICULTURAL FIELDS, 30° INCIDENCE.

Mission 133 June 26, 1970
 Frequency : 13.3 GHz
 Polarization : VV
 θ : 40° Incidence

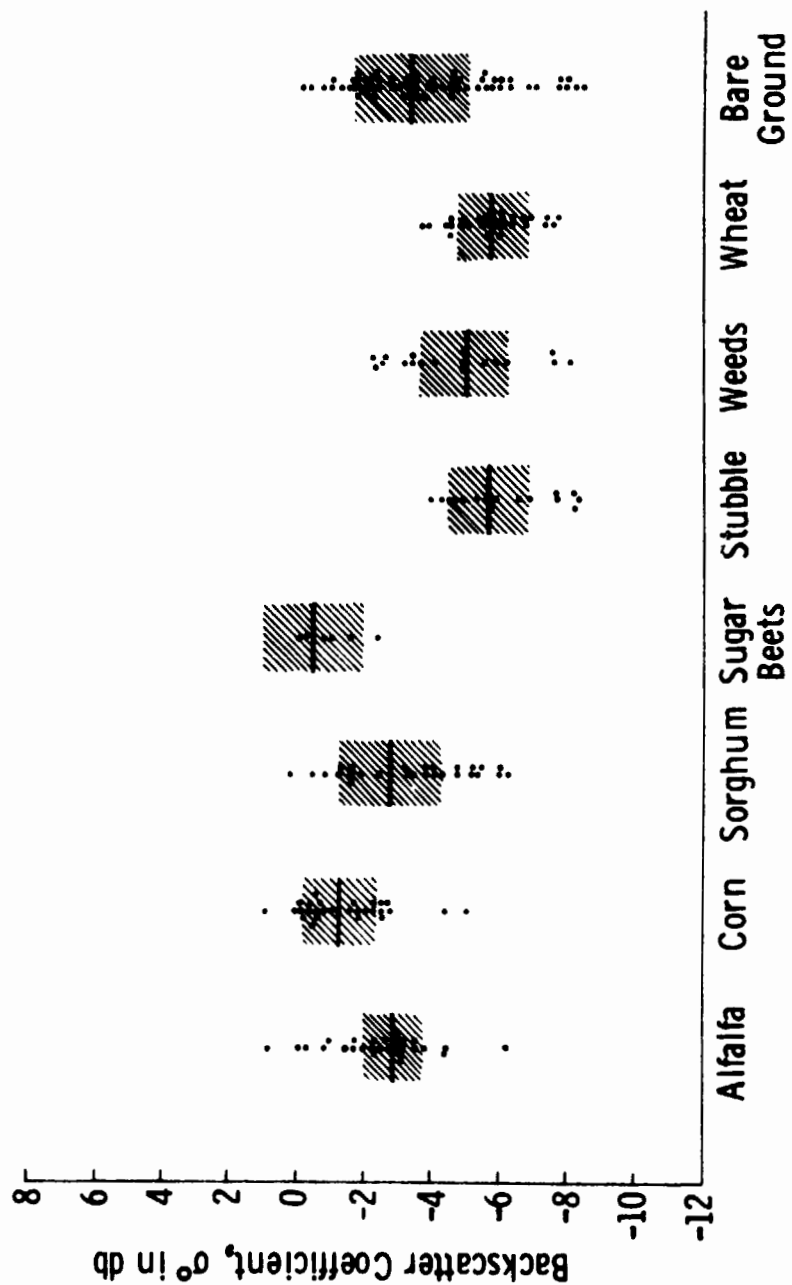


FIGURE 10D. DISTRIBUTION OF MEAN OF AGRICULTURAL FIELDS,
 40° INCIDENCE.

Mission 133 June 26, 1970
 Frequency : 13.3 GHz
 Polarization : VV
 θ : 50° Incidence

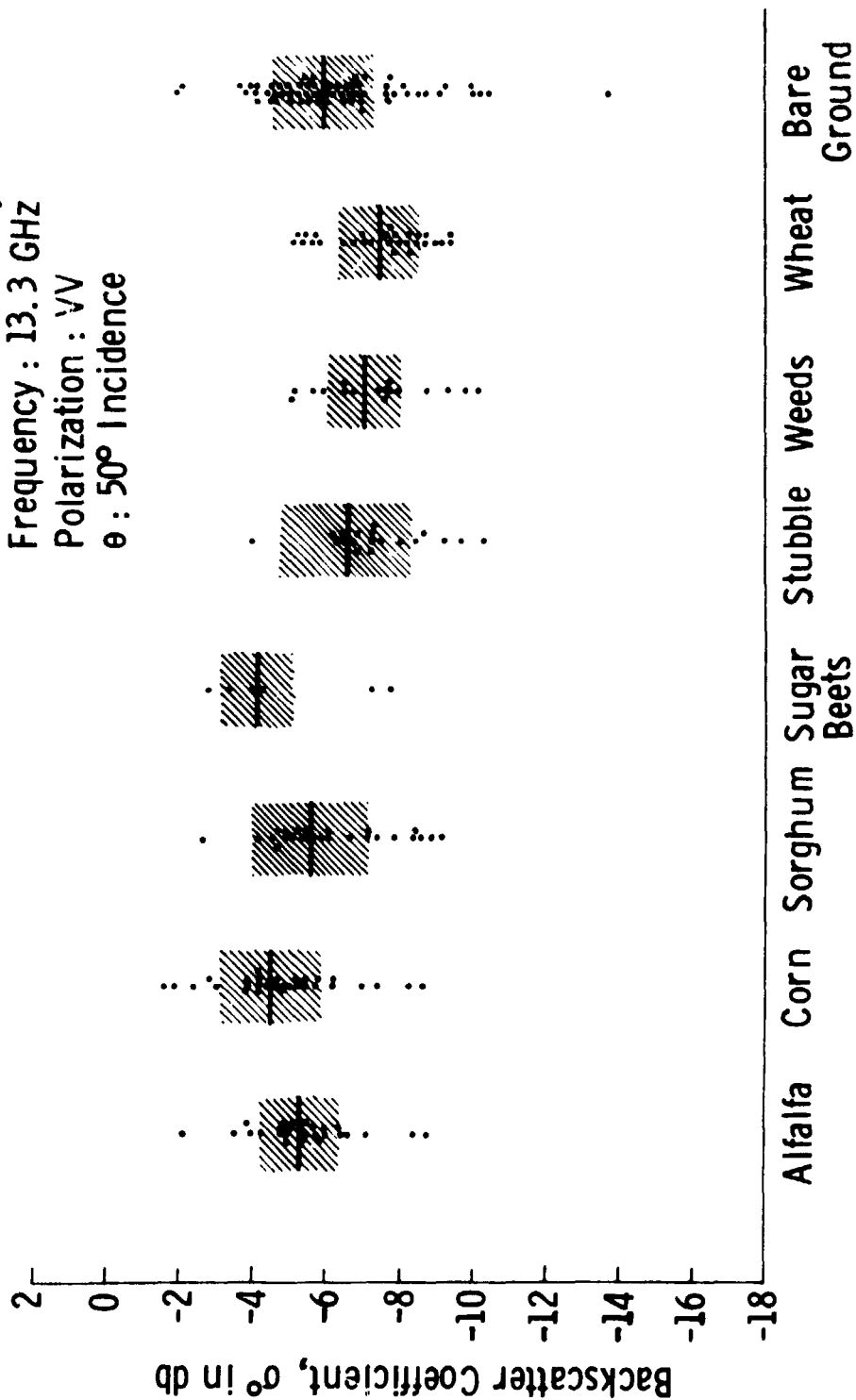


FIGURE 10E. DISTRIBUTION OF MEAN OF AGRICULTURAL FIELDS, 50° INCIDENCE.

Mission 133 June 26, 1970
 Frequency : 13.3 GHz
 Polarization : VV
 θ : 60° Incidence

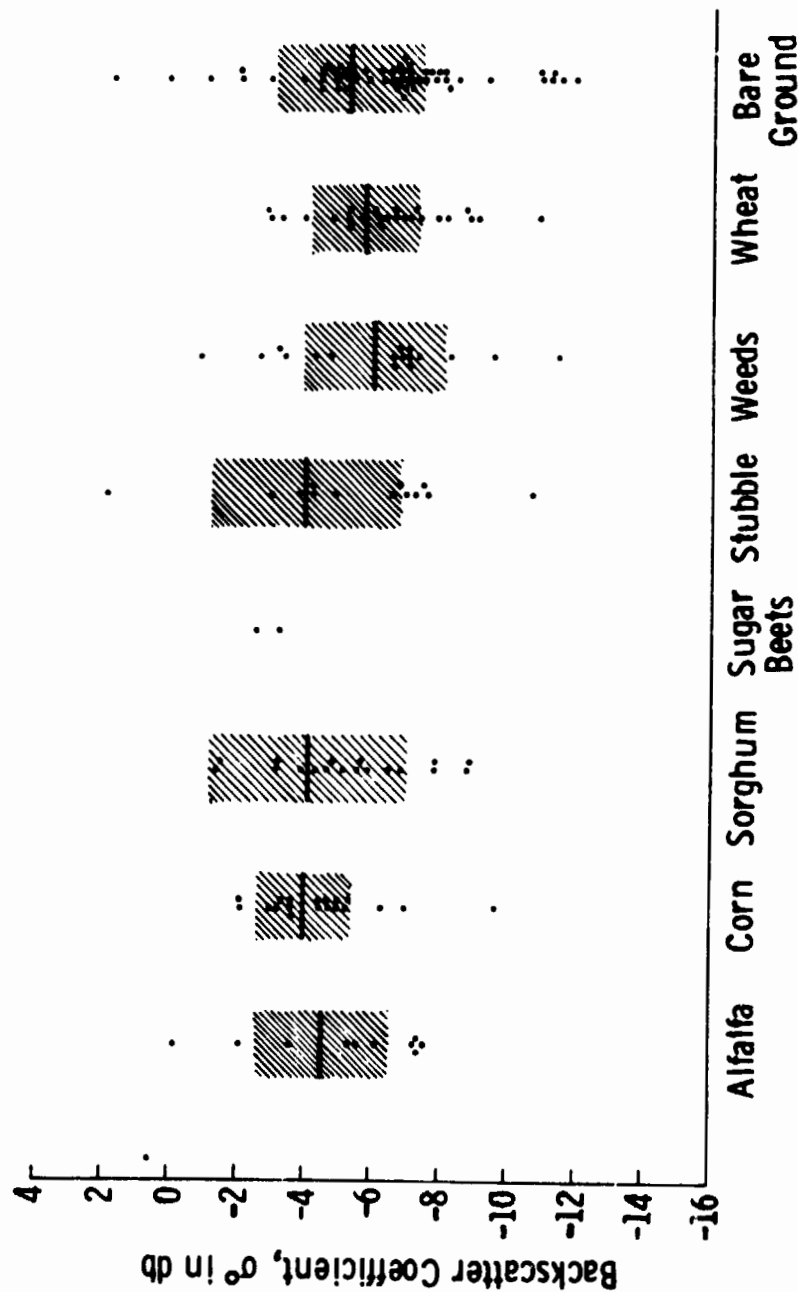


FIGURE 10F. DISTRIBUTION OF MEAN OF AGRICULTURAL FIELDS, 60° INCIDENCE.

MISSION 133 JUNE 26, 1970
 FREQUENCY: 13.3 GHz
 POLARIZATION: VV
 $\theta: 10^\circ$ INCIDENCE

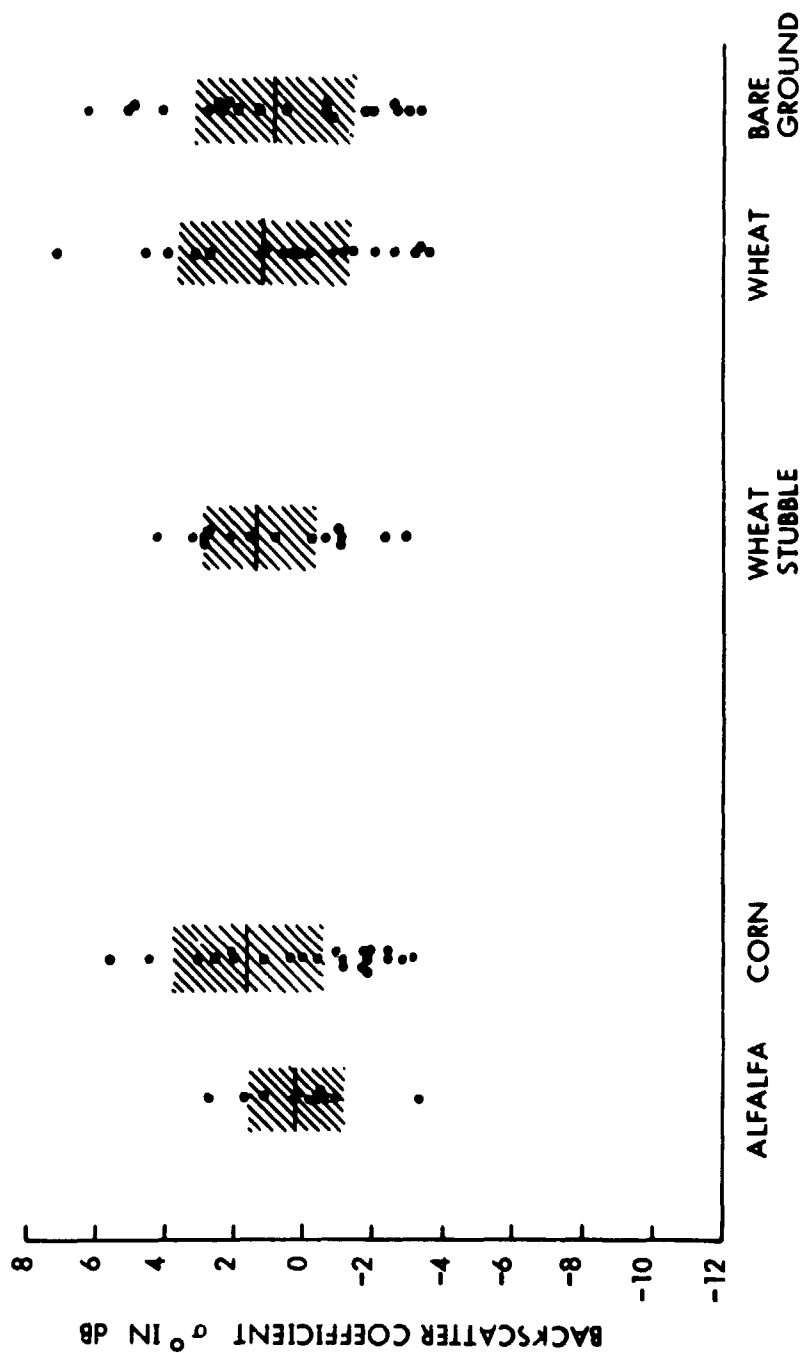


FIGURE 11A. DISTRIBUTION OF STANDARD FARM FIELDS, 10° INCIDENCE.

MISSION 133 JUNE 26, 1970
 FREQUENCY: 13.3 GHz
 POLARIZATION: VV
 θ : 20° INCIDENCE

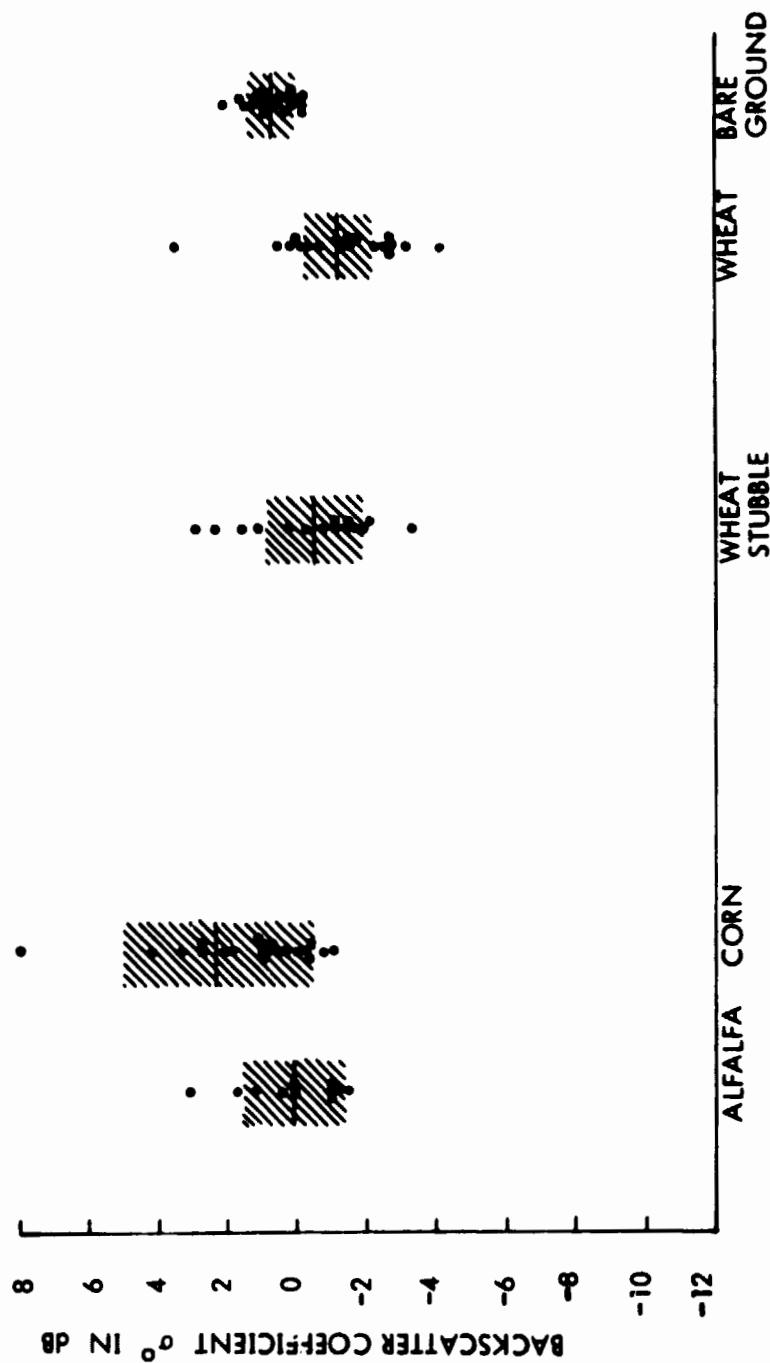


FIGURE 11B. DISTRIBUTION OF STANDARD FARM FIELDS, 20° INCIDENCE.

MISSION 133 JUNE 26, 1970
 FREQUENCY: 13.3 GHz
 POLARIZATION: VV
 θ : 30° INCIDENCE

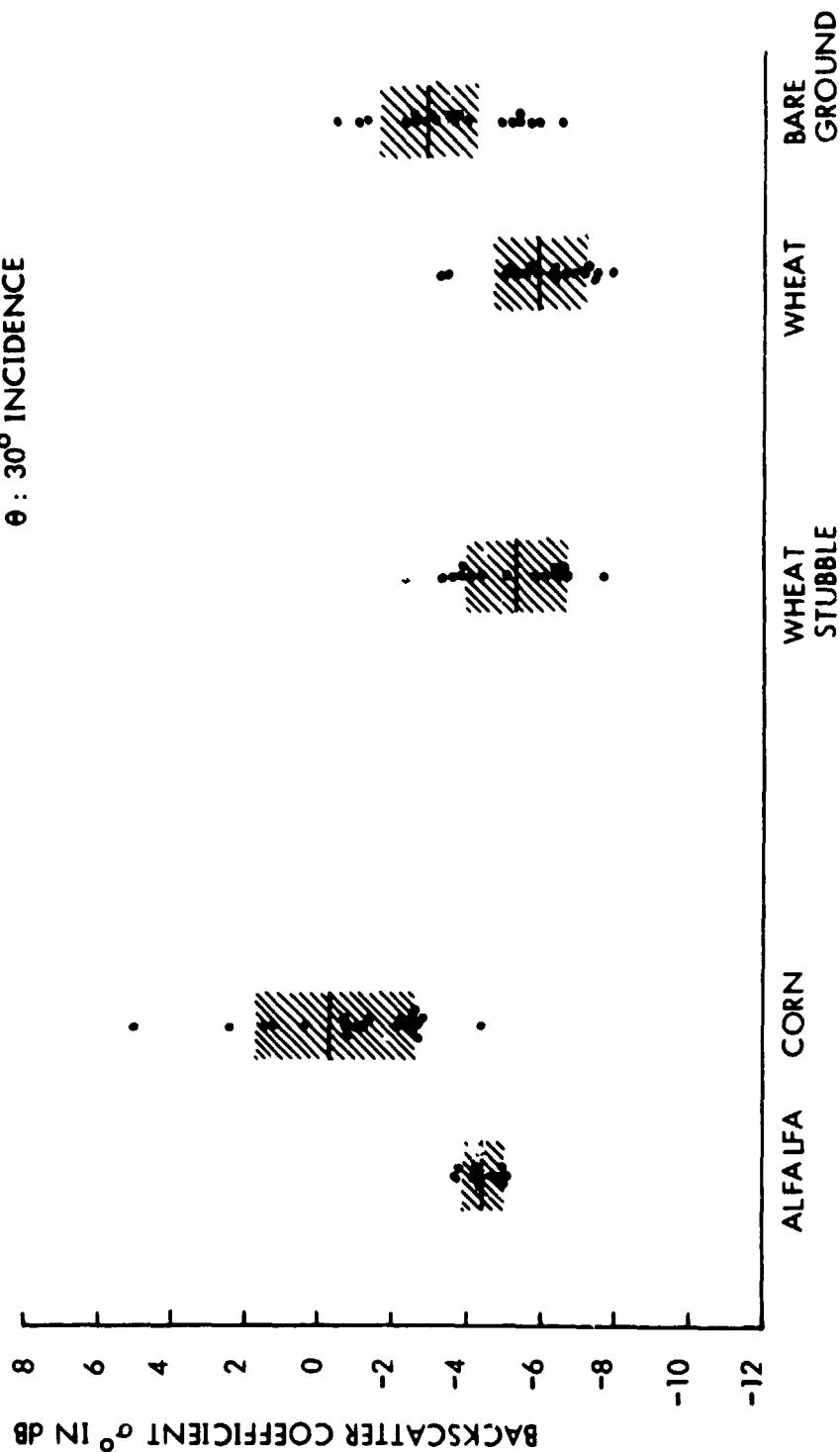


FIGURE 11C. DISTRIBUTION OF STANDARD FARM FIELDS, 30° INCIDENCE.

MISSION 133 JUNE 26, 1970
 FREQUENCY: 13.3 GHz
 POLARIZATION: VV
 θ : 40° INCIDENCE

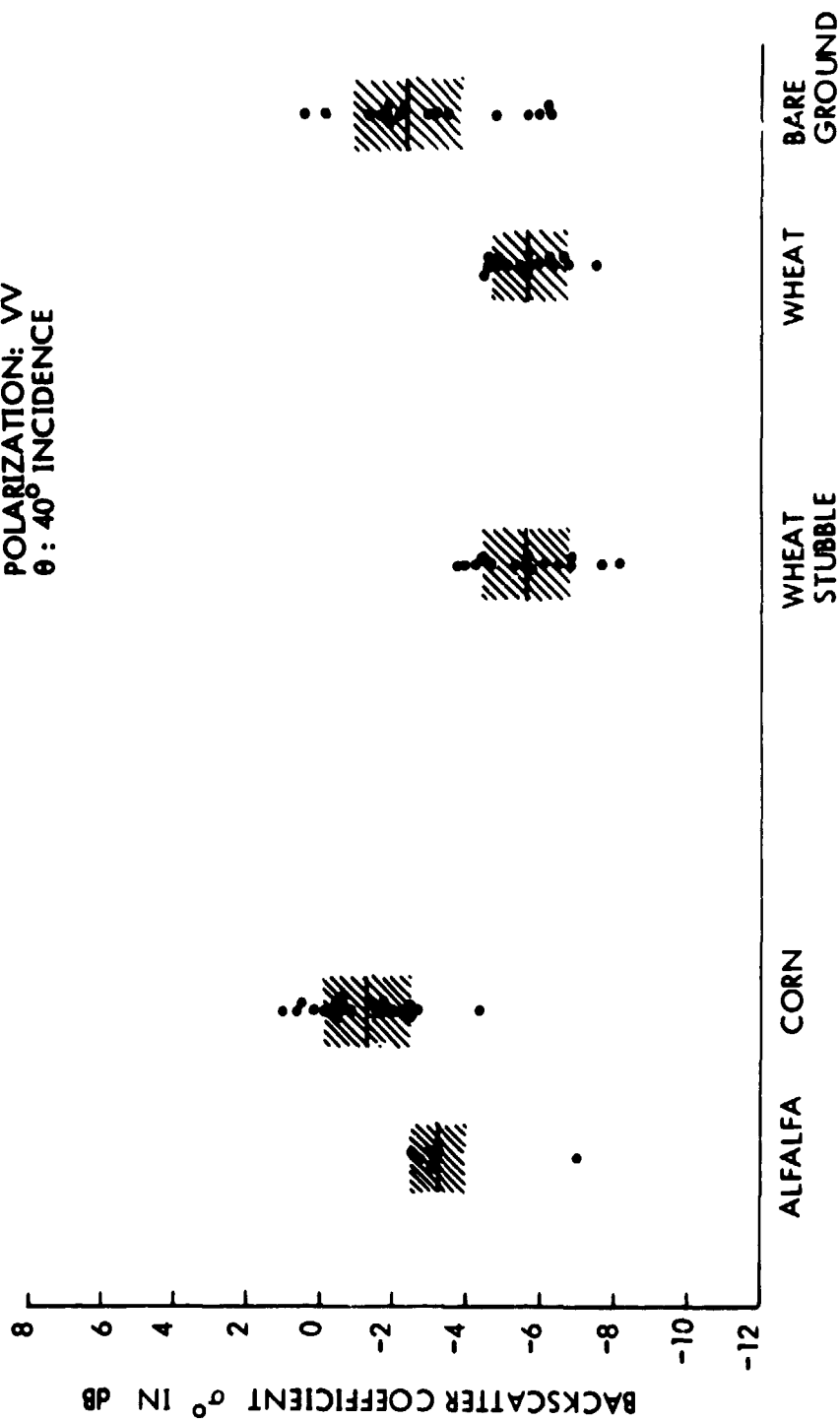


FIGURE 11D. DISTRIBUTION OF STANDARD FARM FIELDS, 40° INCIDENCE.

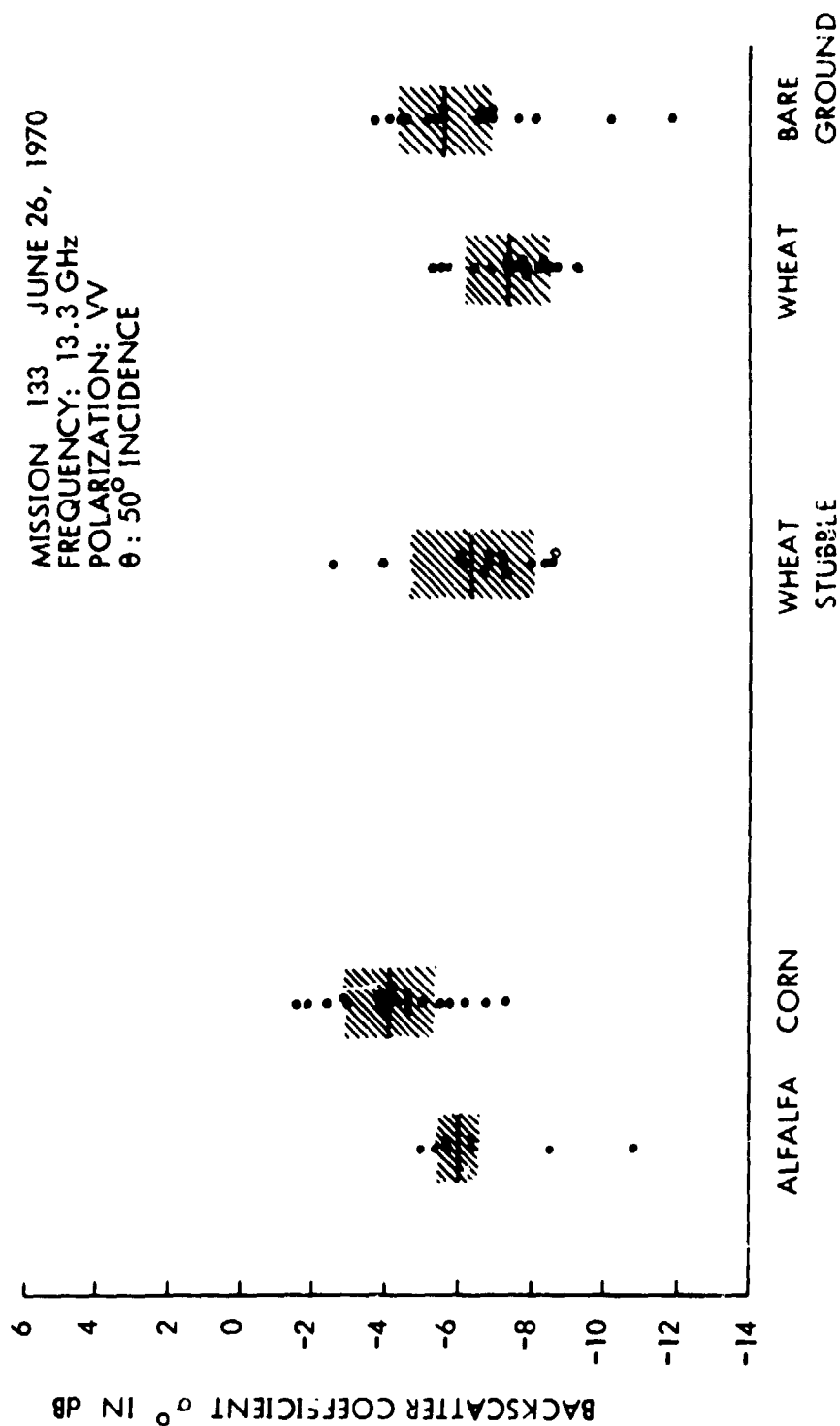


FIGURE 11E. DISTRIBUTION OF STANDARD FARM FIELDS, 50° INCIDENCE.

MISSION 133 JUNE 26, 1970
 FREQUENCY: 13.3 GHz
 POLARIZATION: VV
 θ : 60° INCIDENCE

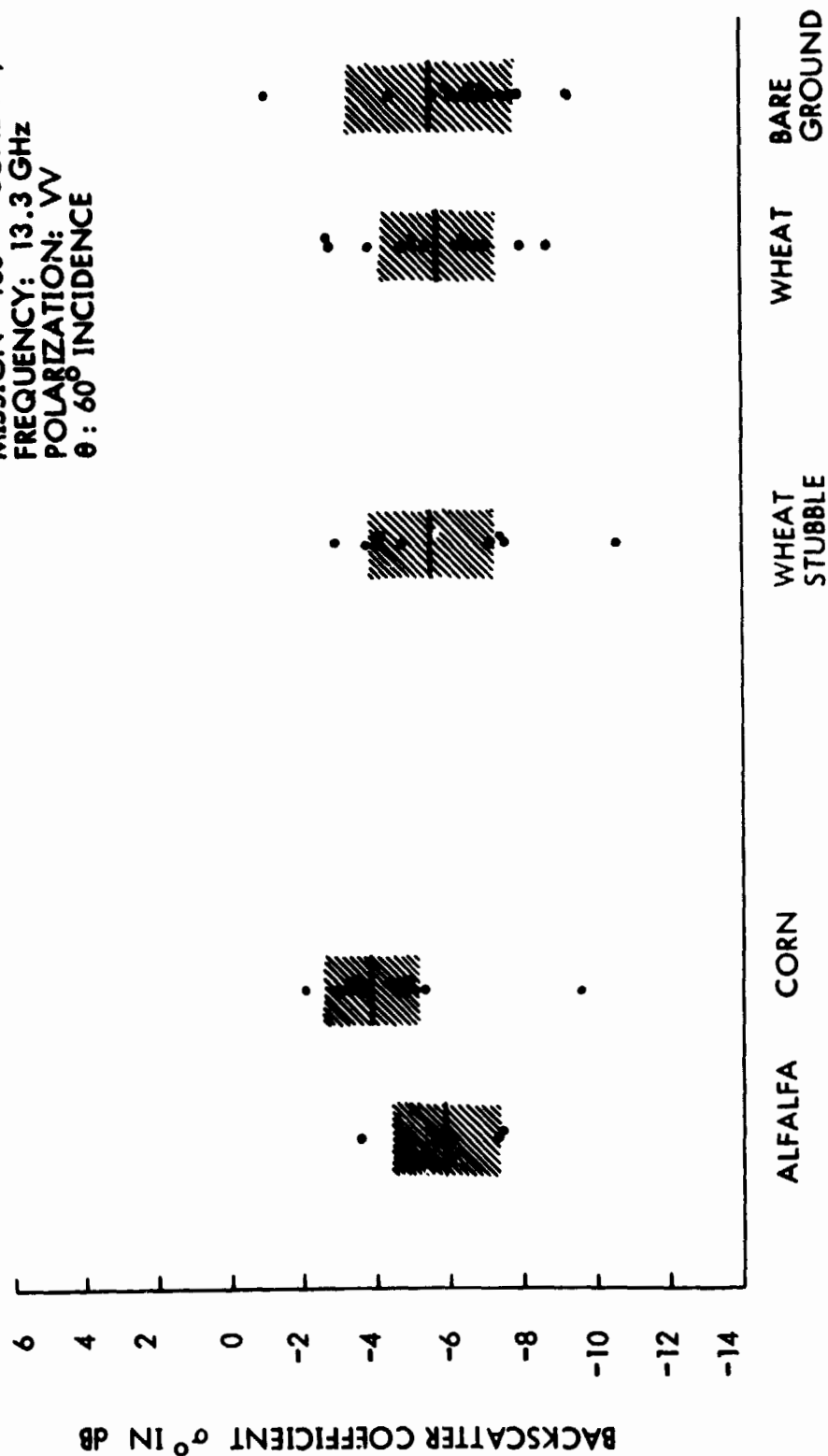


FIGURE 11F. DISTRIBUTION OF STANDARD FARM FIELDS, 60° INCIDENCE.

Other ground parameters which might have accounted for the radar backscatter include plowing pattern, vegetation height and cover, row orientation, ground cracking pattern, clod size, plant moisture content, etc. The only additional parameters considered are ground plowing pattern and vegetation row orientation.

To investigate the variation in radar backscatter caused by a difference in ground plowing direction, bare fields having rows parallel to the scatterometer flight path and rows orthogonal to the flight path were considered. Since the flight path was in a north-south direction, the E-W rows are orthogonal and the N-S rows parallel to the scatterometer look direction. The σ^0 curves for the averaged E-W and N-S oriented fields are shown in Figure 12. The curves cross at 25° incidence but the important fact is the separation between the two curves which is always less than 2 dB. Similarly, vegetated fields have both E-W and N-S planted rows. Figure 13 shows the averaged σ^0 curves of the vegetated fields of orthogonal row direction. The two curves again cross at midrange and the greatest separation between the two is still about 2 dB.

Of the ground parameters investigated so far, soil moisture variation is the major factor contributing to the differences in backscatter at 13.3 GHz. The 400 MHz scatterometer, being multi-polarized, offers an additional system parameter of polarization in the data analysis. Owing to the bulk of the data, the only ground parameter investigated so far is the soil moisture variation.

Some typical 400 MHz curves corresponding to the 13.3 GHz curves of Figure 8 a-c from mission 133 are shown in Figure 14 a-d. These curves, including those not shown, exhibit a difference between corresponding curves for irrigated and non-irrigated fields. However, the magnitude of the difference and the range of incidence angles over which the difference is significant varies much more from field to field than with the 13.3 GHz data. Further, for some fields there are incidence angles at which the two curves cross.

Averaged curves from both missions are shown in Figure 15 a-d. They correspond to Figure 10 a-b of the 13.3 GHz data. A stronger hint of a pattern is present in the averaged 400 MHz curves although it is not as evident as the 13.3 GHz curves.

MISSION 133

SITE GARDEN CITY, KANSAS

FREQUENCY 13.3 GHz

DATE JUNE 26, 1970

POLARIZATION VV

FLIGHT DIRECTION N-S

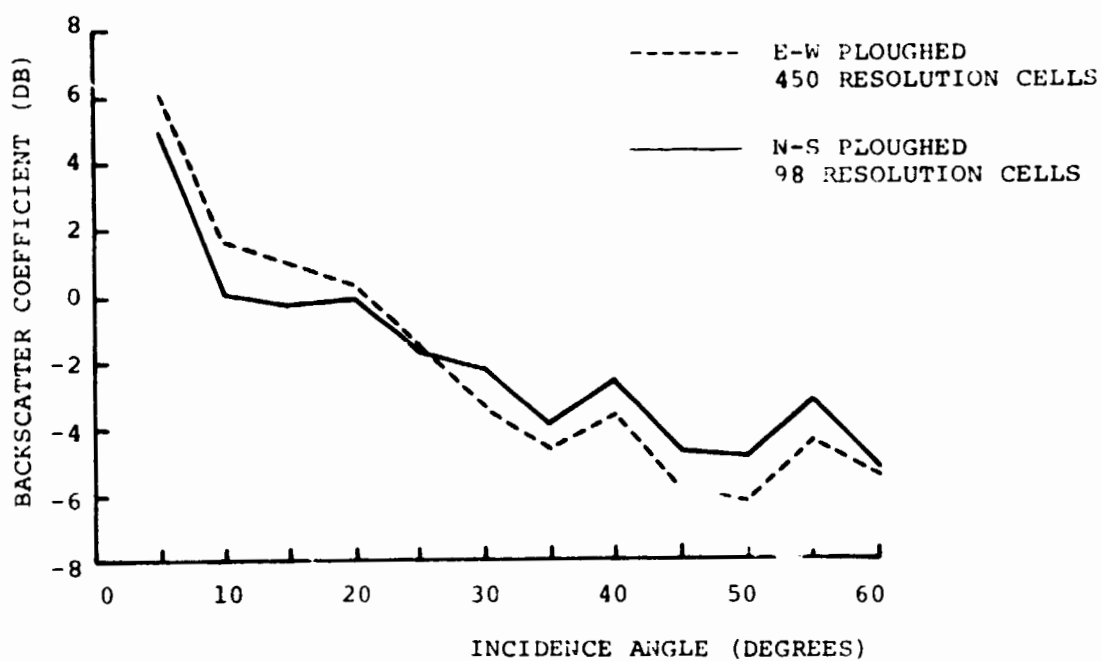


FIGURE 12. BACKSCATTER FOR E-W AND N-S PLOUGHED BARE FIELDS.

S

MISSION 133
FREQUENCY 13.3 GHz
POLARIZATION VV
FLIGHT DIRECTION N-S

SITE GARDEN CITY, KANSAS
DATE JUNE 26, 1970

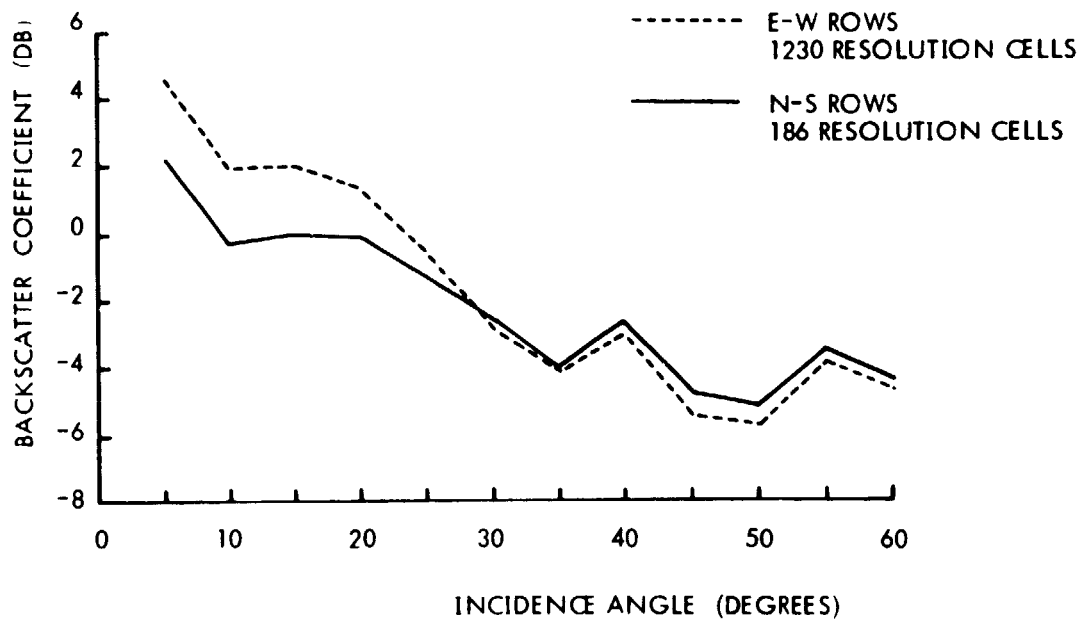


FIGURE 13. BACKSCATTER FOR E-W PLANTED AND N-S PLANTED VEGETATION.

MISSION 133
FREQUENCY 400 MHz
POLARIZATION VV

SITE GARDEN CITY, KANSAS
DATE JUNE 26, 1970
FIELD 27

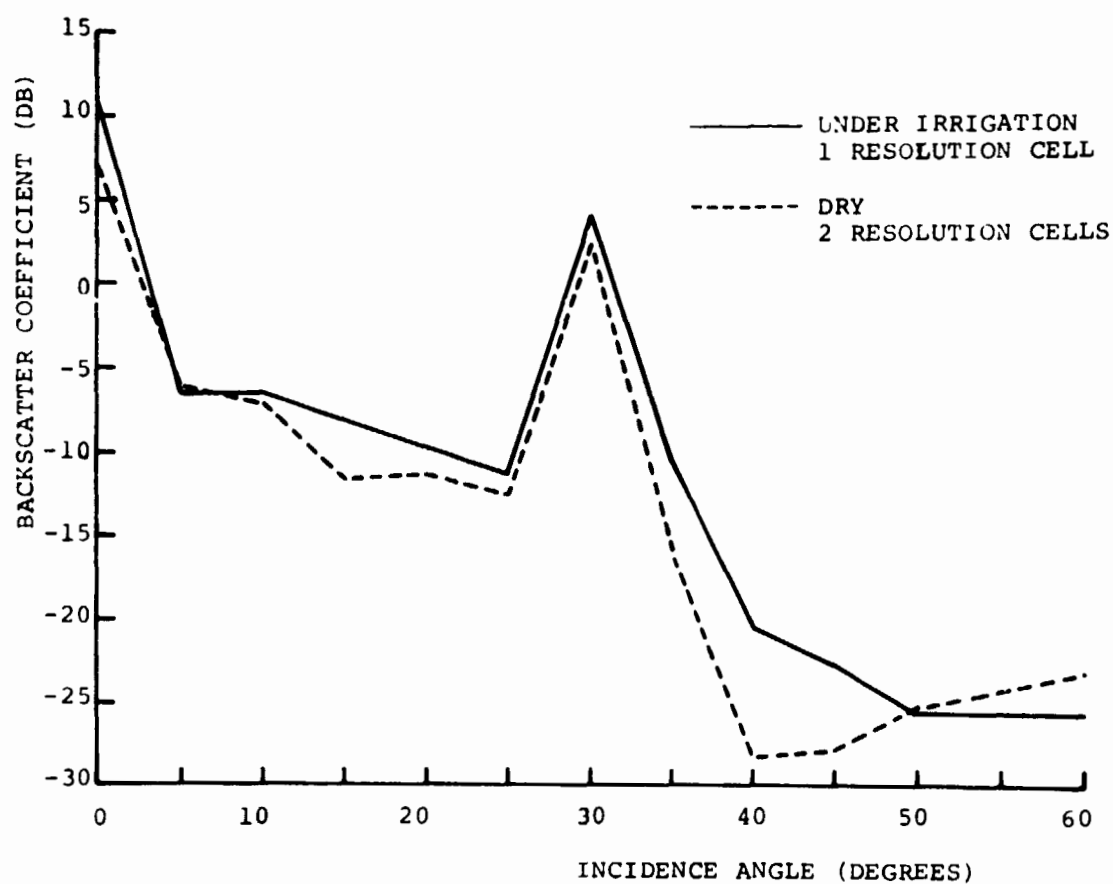


FIGURE 14A. CORN, 36 INCHES, P-BAND, VV POLARIZATION.

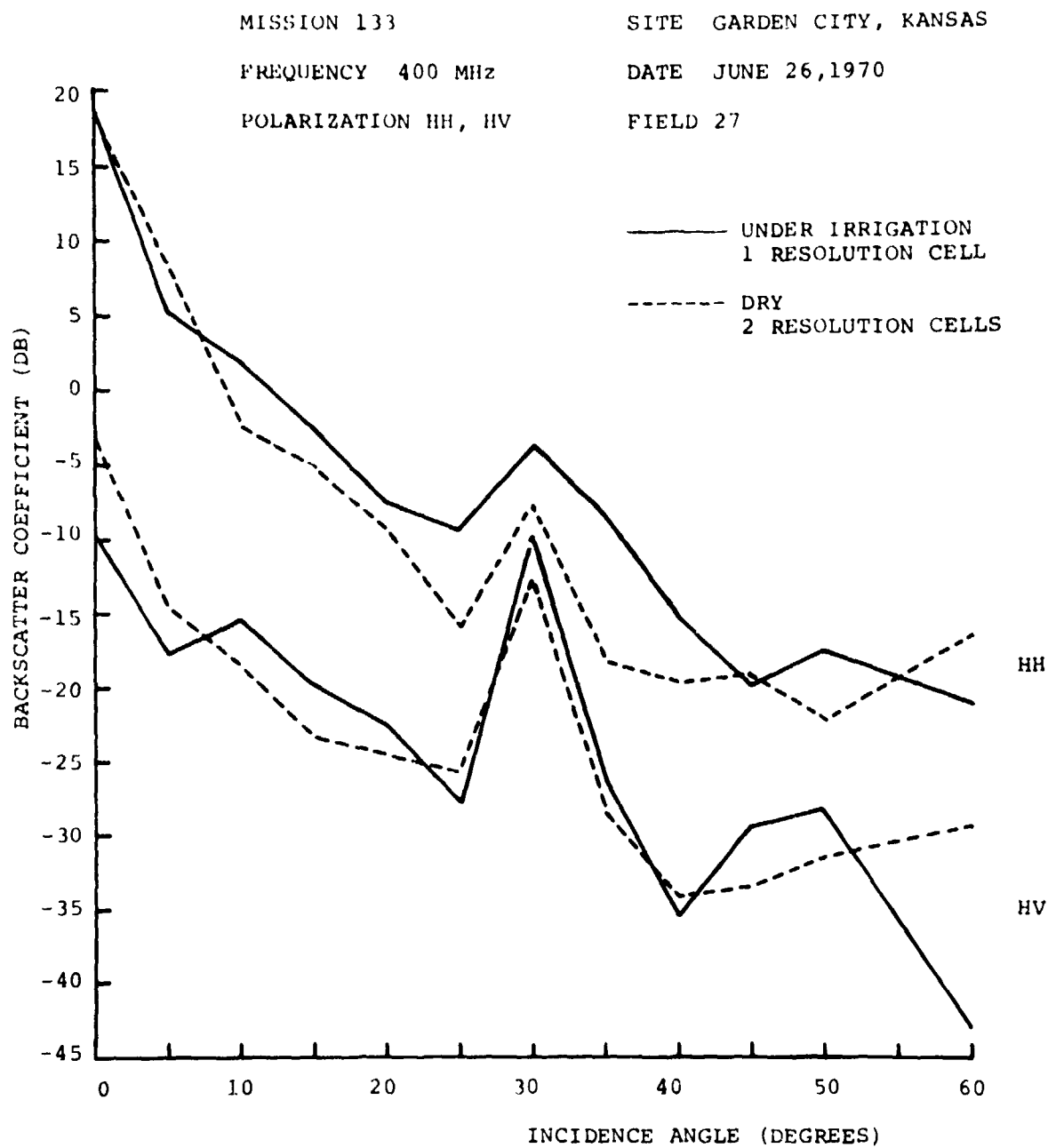


FIGURE 14B. CORN, 36 INCHES, P-BAND, HH AND HV POLARIZATION.

MISSION 133
FREQUENCY 400Mhz
POLARIZATION VV

SITE GARDEN CITY, KANSAS
DATE JUNE 26, 1970
FIELD 108A



FIGURE 14C. ALFALFA AND SUGAR BEETS, P-BAND, VV POLARIZATION.

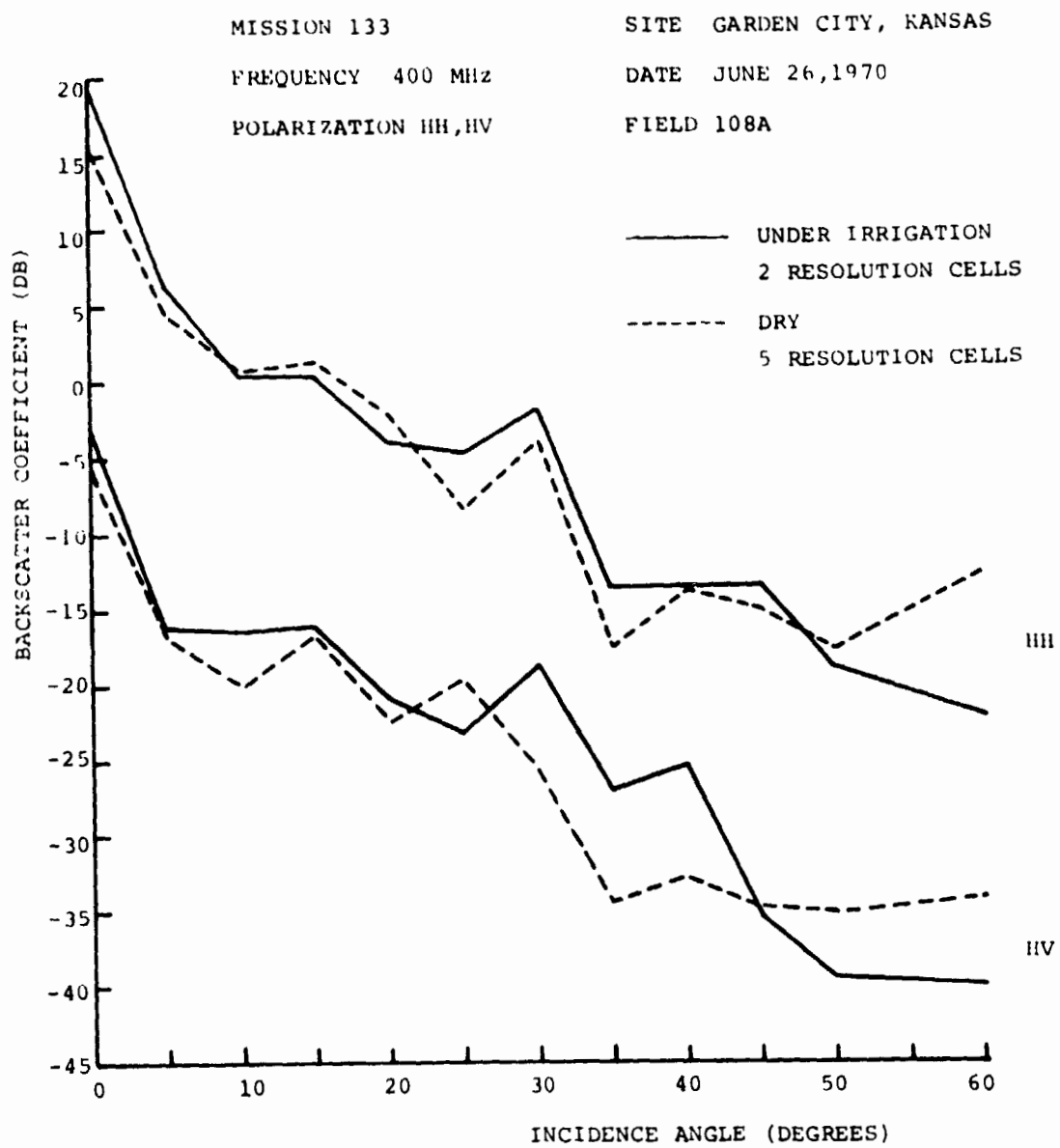


FIGURE 14D. ALFALFA AND SUGAR BEETS, P-BAND, HH AND HV POLARIZATION.

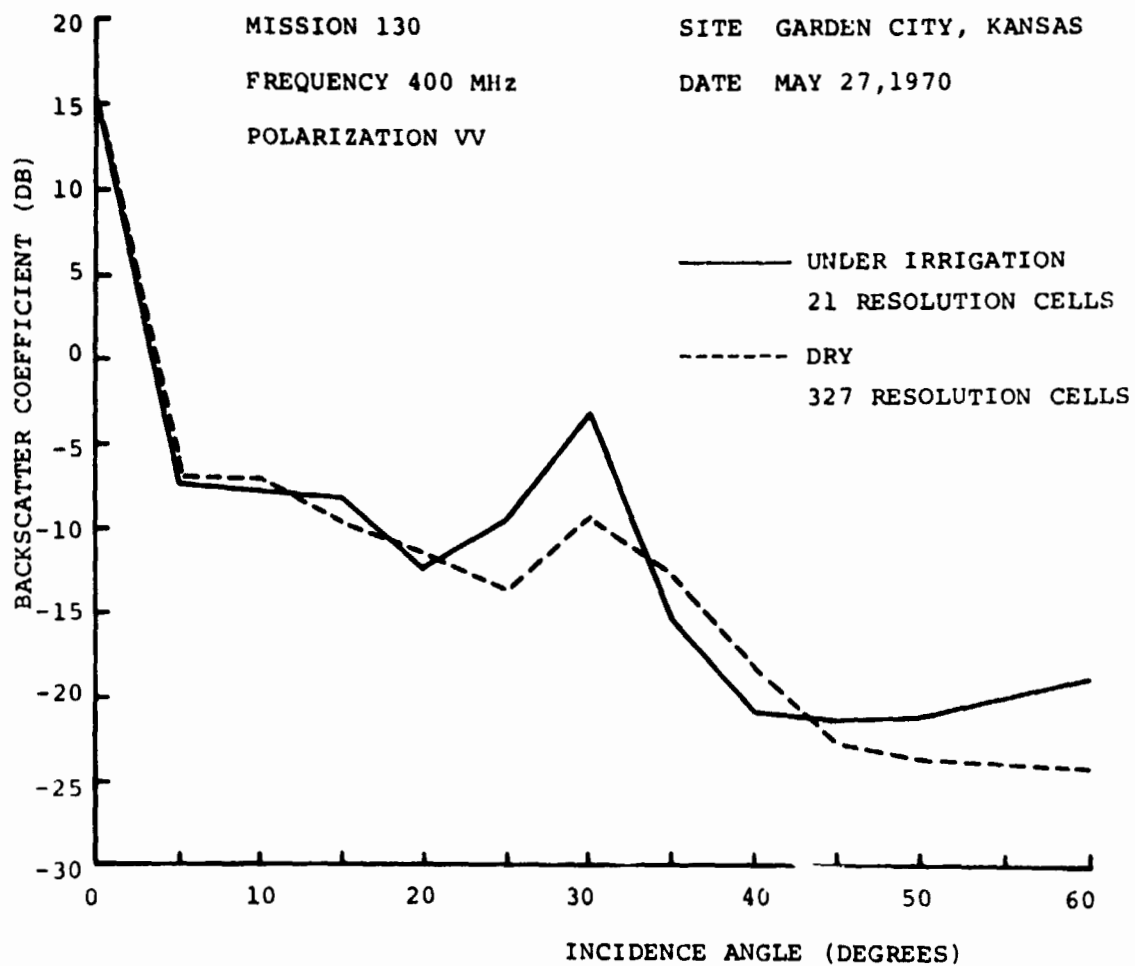


FIGURE 15A. AVERAGE BACKSCATTER FROM MISSION 130 FOR 400 MHZ VV POLARIZATION.

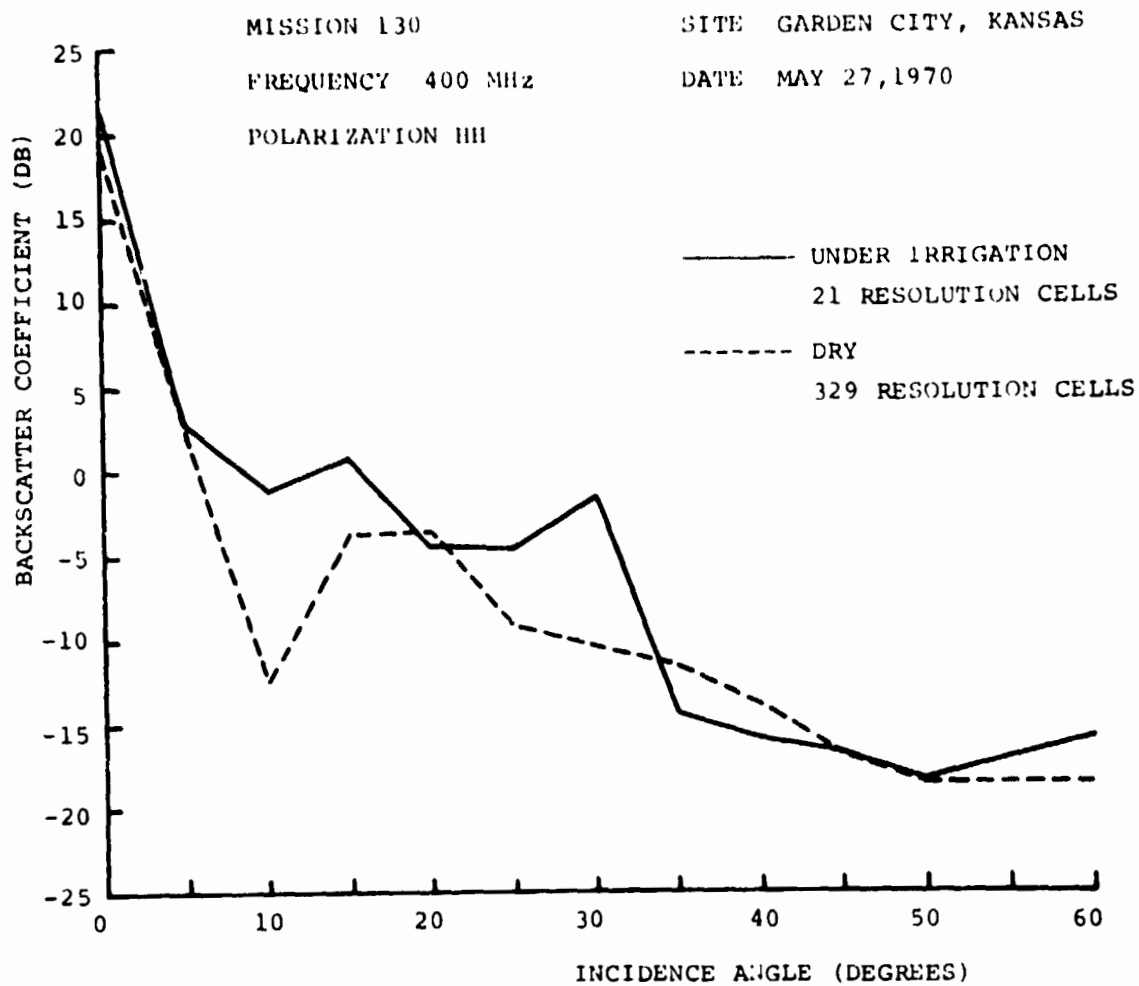


FIGURE 15B. AVERAGE BACKSCATTER FROM MISSION 130 FOR 400 MHZ HH POLARIZATION.

MISSION 130

SITE GARDEN CITY, KANSAS

FREQUENCY 400 MHz

DATE MAY 27, 1970

POLARIZATION HV

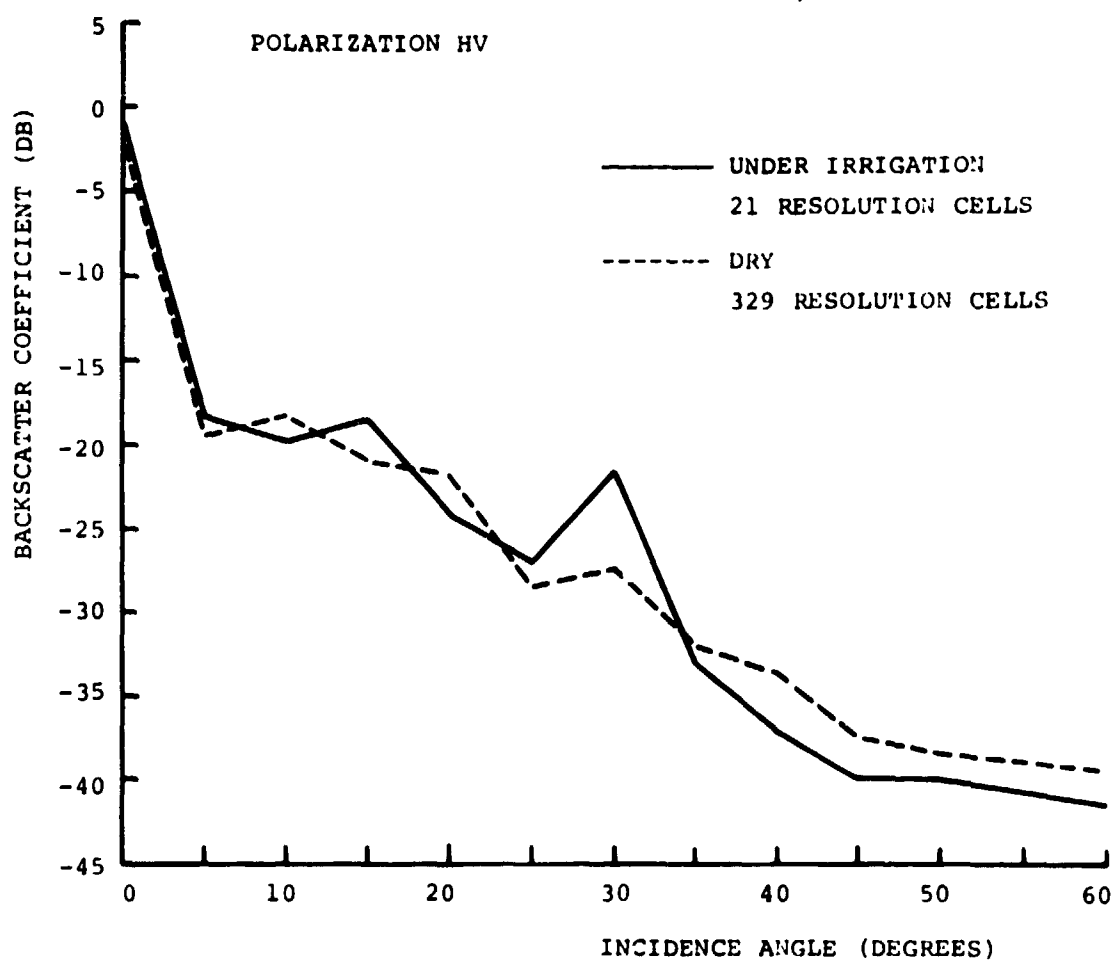


FIGURE 15C. AVERAGE BACKSCATTER FROM MISSION 130 FOR 400 MHZ HV POLARIZATION.

MISSION 133

SITE GARDEN CITY, KANSAS

FREQUENCY 400 MHz

DATE JUNE 26, 1970

POLARIZATION VV

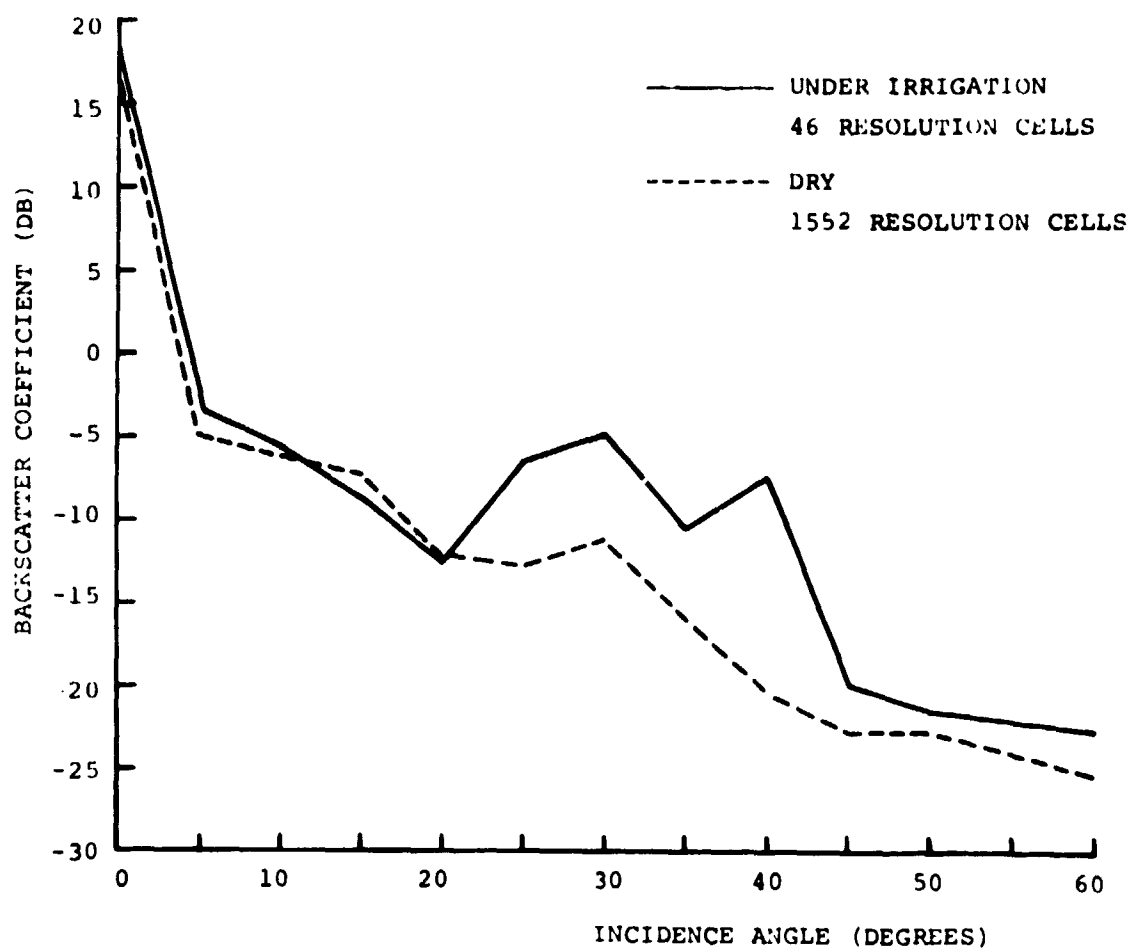


FIGURE 15D. AVERAGE BACKSCATTER FROM MISSION 133 FOR 400 MHZ VV POLARIZATION.

MISSION 133

SITE GARDEN CITY, KANSAS

FREQUENCY 400 MHz

DATE JUNE 26, 1970

POLARIZATION HH

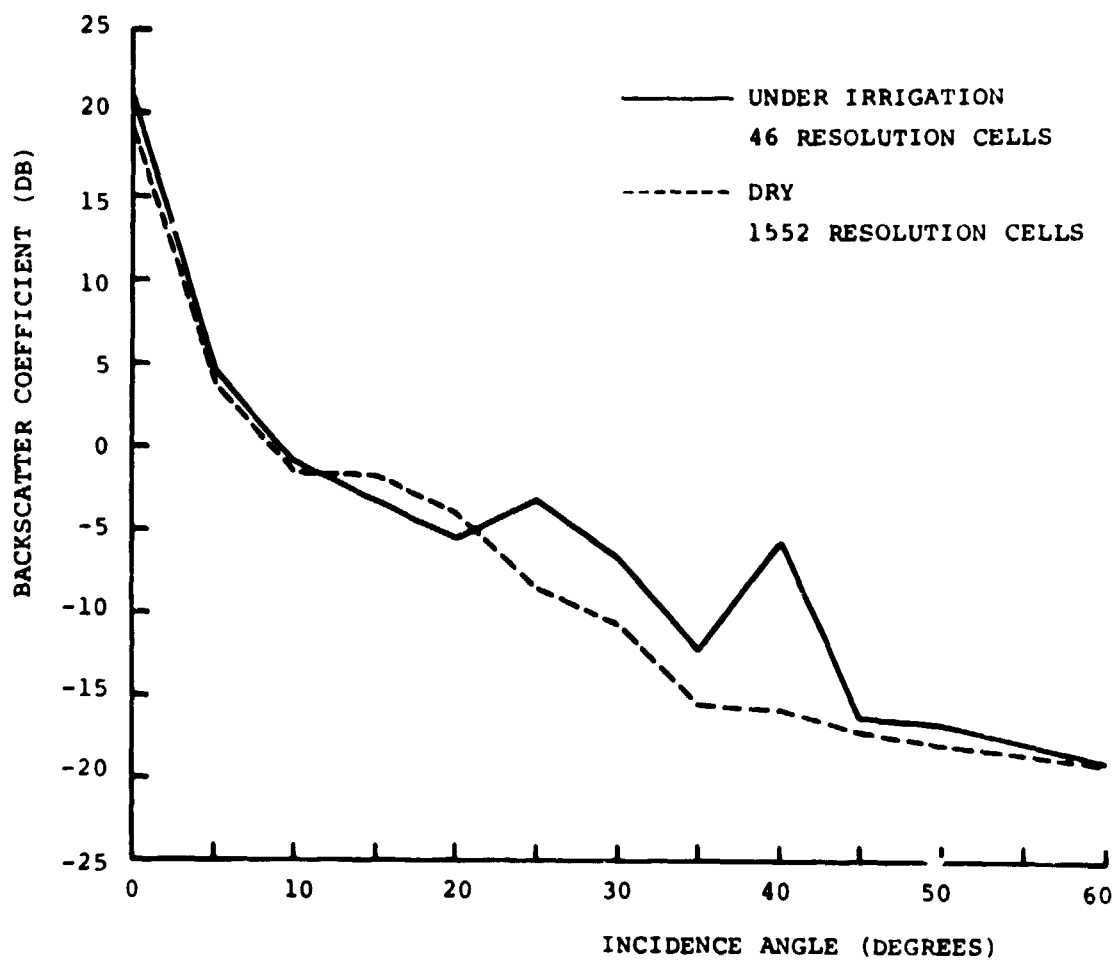


FIGURE 15E. AVERAGE BACKSCATTER FROM MISSION 133 FOR 400 MHZ HH POLARIZATION.

CONCLUSION

The analysis so far has clearly shown the significant dominance of the moisture variation on the backscatter at 13.3 GHz and weaker but still observable dependency at 400 MHz.

For incidence angles less than 40° , the 13.3 GHz data shows a difference in backscatter from wet and dry fields of the order of 7 dB. The differences caused by variations in other ground parameters are not as significant. Analysis shows the averages of the various crop types that fall within a spread of only 5 dB. Other ground parameters such as cultivation pattern and vegetation row effects have even less distinguishing characteristics on the backscatter. Many questions, especially those that deal with specific shape and slope of the σ° curves, are still unanswered. For example, Figure 9 and 10 suggest a slope dependence that might be associated with particular ground treatment and clod size; vegetation height and percent coverage might have influenced the shapes of the curves in Figure 8 a-c. Conclusive statements, however, can only be made after further analysis.

At this point few statements can be made of the 400 MHz data other than to note the slight moisture dependency. Row direction, however, is expected to influence the data more at this longer wavelength.

These data are only for June and, at 13.3 GHz, for VV polarization. General conclusions applicable to other months or polarizations should be avoided insofar as vegetation echo is concerned. Presumably the conclusions regarding soil moisture effects are more general.

REFERENCES

1. Spurr, S. H., Photogrammetry and Photo-interpretation, Ronald Press Co., New York, 2nd edition, pp. 289-290, 1960.
2. Edgerton, A. T., "Engineering Application of Microwave Radiometry," Proc. 5th Symposium on Remote Sensing of Environment, University of Michigan, Ann Arbor, pp. 711-724, April, 1969.
3. Hruby, R. J. and A. T. Edgerton, "Subsurface Discontinuity Detection by Microwave Radiometry," Proc. 7th Symposium on Remote Sensing of Environment, University of Michigan, Ann Arbor, pp. 319-325, May, 1971.
4. MacDonald, H. C. and W. P. Waite, "Soil Moisture Detection with Imaging Radar," Water Resources Research, vol. 7, no. 1, pp. 100-110, February, 1971.
5. Lundien, J. R., "Terrain Analysis by Electromagnetic Means, Report 2, Radar Responses to Laboratory Prepared Soil Samples," U. S. Army Eng. Waterways Expt. Sta. Tech. Rept. 3-693, Vicksburg, Mississippi, pp. 1-55, September, 1966.
6. Dickey, F., C. King, J. Holtzman and R. K. Moore, "Moisture Dependency of Radar Backscatter from Irrigated and Non-Irrigated Fields at 400 MHz and 13.3 GHz," University of Kansas Center for Research Inc., CRES Technical Memorandum 177-33, Lawrence, Kansas, September, 1972, also to be published in IEEE Trans. Geoscience Electronics, January, 1974.
7. Moore, R. K., "Radar Scatterometry—An Active Remote Sensing Tool," Proc. 4th Symposium on Remote Sensing of Environment, University of Michigan, Ann Arbor, pp. 339-375, April, 1966.
8. Moore, R. K., "Ground Echo," in Skolnik, M. I. (ed), Radar Handbook, McGraw-Hill, New York, 1970.
9. Boles, W. D., "Scattering of Waves from a Rough Layer," University of Kansas Center for Research, Inc., CRES Technical Report 118-19, Lawrence, Kansas, December, 1969.
10. Moore, R. K., "Use of Microwaves for Snow, Freeze-thaw, and Soil Moisture Determination—A Needed Research Program," University of Kansas Center for Research, Inc., CRES Technical Memorandum 100-1, Lawrence, Kansas, February, 1972.
11. Carlson, N. L., "Dielectric Constant of Vegetation at 8.5 GHz," Ohio State University Electro-Science Lab Technical Report 1903-5, Columbus, Ohio, 1967.

12. Barrick, D. E. and W. H. Peake, "Scattering from Rough Surfaces with Different Roughness Scales: Analysis and Interpretation," Ohio State University Electro-Science Lab Technical Report 1388-26, Columbus Ohio, 1967.
13. Emerson Electric Co. Electronics and Space Division, "400 MHz Scatterometer—Final Report," under contract NAS 9-6742, Houston, Texas, December 1968.
14. Moore, R. K. and W. P. Waite, "Radar Scatterometry," University of Kansas Center for Research, Inc., CRES Technical Report 118-15, Lawrence, Kansas, January, 1969.
15. Chan, H. L. and A. K. Fung, "Backscattering from a Two-Scale Rough Surface with Applications to Radar Sea Return," University of Kansas Center for Research, Inc., CRES Technical Report 186-4, Lawrence, Kansas, August, 1971.